REPORT DOCUMENTATION PAGE

AFRL-SR-AR-TR-08-0005

1. REPORT DATE *(DD-MM-YYYY)*	2. REPORT TYPE	3. DATES COVERED *(From - To)*
12/10/07	Final	1/1/06 to 2/1/07

4. TITLE AND SUBTITLE
Molecular Mechanisms of NonLinearity in Response to Low Dose Ionizing Radiation

5a. CONTRACT NUMBER

5b. GRANT NUMBER
FA9550-06-1-0132

5c. PROGRAM ELEMENT NUMBER

6. AUTHOR(S)
Zelanna Goldberg and David M. Rocke

5d. PROJECT NUMBER

5e. TASK NUMBER

5f. WORK UNIT NUMBER

7. PERFORMING ORGANIZATION NAME(S) AND ADDRESS(ES)
University of California,
Davis
Dept of Public Health

8. PERFORMING ORGANIZATION REPORT NUMBER

9. SPONSORING / MONITORING AGENCY NAME(S) AND ADDRESS(ES)
AFOSR/NL
AFOSR/NL
875 North Randolph Street
Suite 325, Room 3112
Arlington, CA 22203-1768

10. SPONSOR/MONITOR'S ACRONYM(S)

11. SPONSOR/MONITOR'S REPORT NUMBER(S)

12. DISTRIBUTION / AVAILABILITY STATEMENT
Approve for public release, distribution unlimited.

13. SUPPLEMENTARY NOTES

14. ABSTRACT
In this very new project we have begun a systematic evaluation of the molecular mechanisms of radiation adaptation. We have developed a wound-healing model that will provide a functional assessment of the promitogenic effects of low dose radiation exposure. We have begun detailed cell cycle analysis of low dose radiation exposure on human keratinocytes and fibroblasts as well as survival assays following priming and challenge doses of ionizing radiation. Initial experiments suggest that doses in the range of 10 cGy provide a promitogenic signal. Further, a priming dose of 10-20 cGy seems to provide radiation protection against subsequent challenge doses up to 4 Gy. Beyond 4 Gy in challenge doses, the radioprotective effect of the priming dose seems to be overwhelmed. Genomic evaluation using the Illumina microarray platform is ongoing.

15. SUBJECT TERMS

16. SECURITY CLASSIFICATION OF:			17. LIMITATION OF ABSTRACT	18. NUMBER OF PAGES	19a. NAME OF RESPONSIBLE PERSON
a. REPORT	b. ABSTRACT	c. THIS PAGE			19b. TELEPHONE NUMBER *(include area code)*

Grant Title: Molecular Mechanisms of NonLinearity in Response to Low Dose Ionizing Radiation
Grant #: FA9550-06-1-0132
Reporting Period: 1/1/06 – 2/1/07

Institution: University of California, Davis

Investigators: Zelanna Goldberg, MD
David M. Rocke, PhD
Department of Public Health Sciences
University of California, Davis

Technical Summary:

Summary of Papers

Goldberg, Z., Rocke, D., Schwietert, C., Berglund, S., Santana, A., Jones, A., Lehmann, J., Stern, R., Lu, R., Hartmann-Siantar, C. (2006) Human in vivo dose-response to controlled, low-dose low linear energy transfer ionizing radiation exposure. Clin Cancer Res., 12, 3723–3730.

This paper is the first to describe transcriptional responses to low-dose ionizing radiation in vivo in humans. The earlier dosimetry work allowed for accurate quantitation of precisely calibrated doses which were verified by TLD's and MOSFETs. Eight men were included in this study, a biopsy was taken prior to each patient's first radiation treatment and three biopsies were taken 3 hours post exposure at locations on the abdomen which received 1, 10 or 100 cGy doses. Each biopsy was processed and the RNA was interrogated on an Affymetrix HGU133 Plus 2.0 array. The data was analyzed using the method of Rocke et al as described above, which determined significant differential expression of pre-selected gene groups and pathways. The results identified seven of nineteen gene groups and five of seven gene pathways which were up or down regulated. The gene groups up regulated included: BCL6, cytokines, mitogen-activated protein kinases, and zinc finger proteins. The gene groups down regulated included: keratins, protein disulfide isomerase and S100. The five pathways all displayed up regulation and included: transforming growth factor β/cyclin/ubiquitin pathway, stress/apoptosis, inflammation, growth factor/insulin, and AKT/phosphoinositide-3-kinase. The gene groups and pathways found in this study have known functions in apoptosis, cell cycle arrest, DNA repair and inflammation. This indicates that the skin responds to the injury, initiates a stress/inflammatory response, enhances survival and begins DNA damage repair. These data show that there is a definable response in three dimensional, full thickness, in vivo tissue to LDIR.

Berglund, S.R., Rocke, D.M., Dai, J., Schweitert, C., Santana, A., Stern, R., Lehman, J., Hartmann Siantar, C., and Goldberg, Z. (2007) Transient genome-wide transcriptional response to low-dose ionizing radiation in-vivo in humans, International Journal of Radiation Oncology, Biology, Physics, in press.

This is our second published paper using our developed methodology and is the first report to describe the temporal transcriptional changes found in response to low dose ionizing radiation in vivo in humans. A different cohort of men was used in this study and biopsies were taken at 10 cGy location before treatment at time 0 and at 3, 8 and 24 hours post exposure. We compared the 0 and 24 hour samples to the 3 and 8 hours samples to determine transient responses. To summarize, we assumed that responses seen in the 3 and 8 hour biopsies could be considered transient responses if they returned to the baseline seen in the control biopsy by the 24 hour time point. Using the same gene group and pathway probe sets, we found that 9 gene groups showed transient expression. Groups that were up-regulated included: zinc finger proteins, keratins, BMP receptors, BAG, and cyclins. Down-regulated groups included: TNF, interleukins, heat shock proteins and S100 proteins. None of the pathways showed transient regulation suggesting that the tissue response is sustained past the 24 time point in this data set. The response of the gene groups over time indicate that tissue repair and DNA remodeling are acute and may be completed in the first 24 hours post exposure. The decrease in TNF and interleukins suggests that the stress response is dimished while the tissue attempts to repair DNA and other damage. A response of this type is considerably different that what has been seen in high dose exposures, and supports the findings of other recently emerging in vitro data.

Susanne R. Berglund, Alison Santana, Dan Li, David Rocke, and Zelanna Goldberg, "Proteomic Analysis of Low Dose Arsenic and Ionizing Radiation Exposure on Keratinocytes," submitted for publication.

The human health effects of arsenic and ionizing radiation at environmental levels have been examined separately, but little information regarding potential interactions at low doses exist. Arsenic toxicity may be synergistically affected by concurrent low dose ionizing radiation especially in light of their known individual carcinogenic actions at higher doses. A proteomics approach was used to examine the interaction of ionizing radiation and arsenic in a human cell line. Exposure resulted in differential proteomic expression. Based on MSMS, immunoblotting and statistical analysis (ANOVA); thirteen proteins were identified including: annexin XI, calmodulin, cyclophilin A, α-enolase, epidermal fatty acid-binding protein (E-FABP), heat shock protein 27, histidine triad nucleotide-binding protein 1, lactate dehydrogenase A (LDH A), profilin-1, protein disulfide isomerase precursor (PDI), pyruvate kinase M isozyme, R3372_1 and S100A9. Six of the proteins responded to ionizing radiation and eight reacted to arsenic exposure. Four of these proteins, α-enolase, E-FABP, LDH A and PDI had an effect that was different than would be expected based on the effects of either toxicant alone demonstrating a possible response to the combined insult that is substantially different from either separate treatment.

Adaptive Response in Epithelial Tissue

It is known that 85% of cancers originate in epithelial tissues, yet there is little literature on adaptive response in epithelial cells. The most common cell types for adaptive response studies, and studies of low-dose ionizing radiation in general, are fibroblasts, lympocytes, and lymphoblastoid cell lines. A few studies have been conducted on Chinese hampster ovary (CHO) cells, which are fibroblast-like, and neuroblastoid cell lines.

Under the funding from this project, we have begun investigations into adaptive response in epithelial cells (several keratinocyte cell lines), stromal cells (several fibroblast cell lines, and the interactions between them. We have used the MTS assay, a micronuclei assay, and several flow cytometric assays to refine the priming/challenge dose "sweet spot" for adaptive response. Although the data are not yet published, we have good evidence that the optimal priming dose is in the 5–30 cGy range for protection against a variety of challenge doses, depending on the cell type. Illustrative data are shown in the two Figures below.

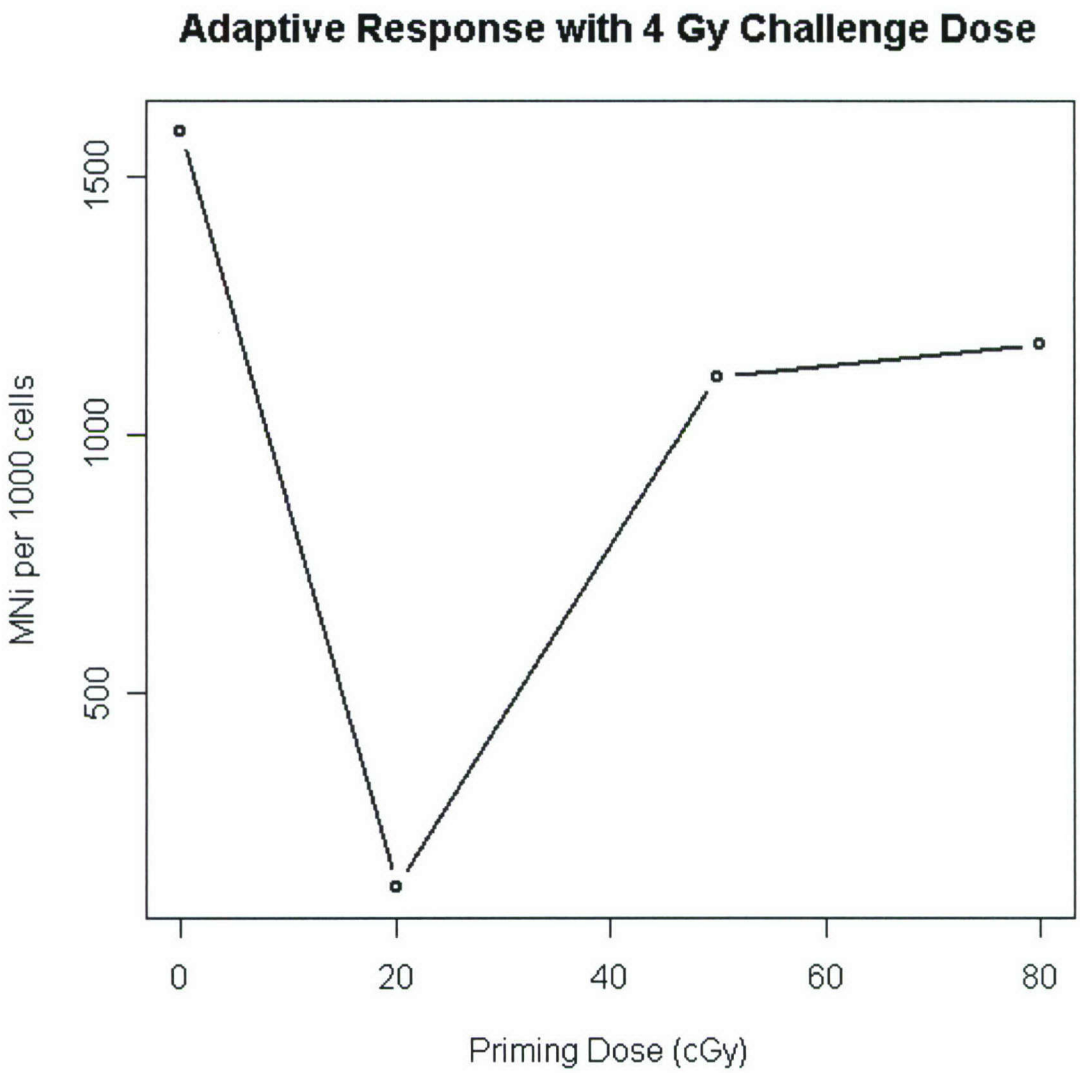

Figure 1. Micronuclei assay results for a keratinocyte cell line (HaCaTs) at priming doses from 0 to 80 cGy showing that the optimal priming dose is probably between 1 and 30 cGy. The results are still preliminary, but have been partially confirmed as shown in Figure 2.

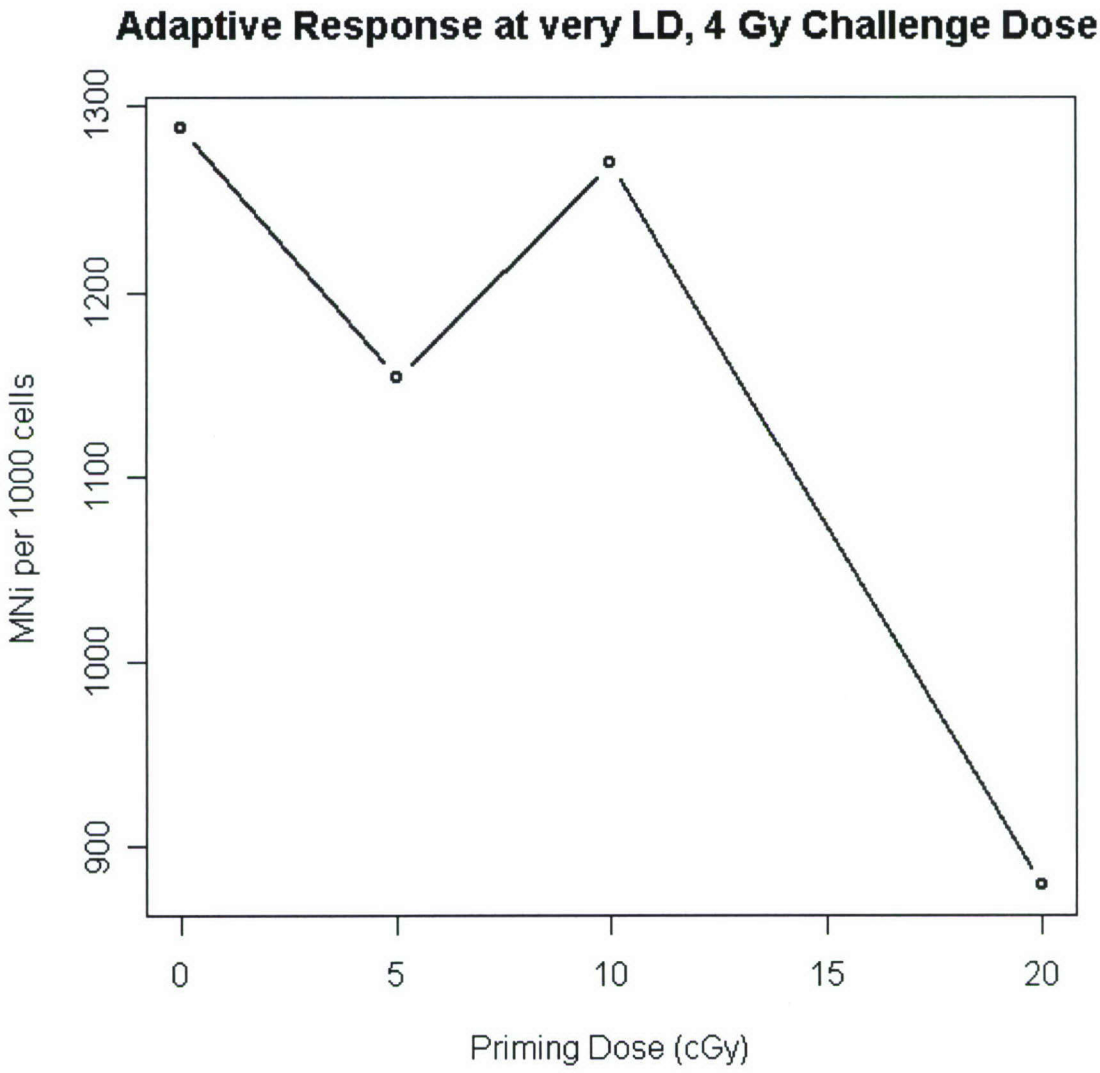

Figure 2. Micronuclei assay results for a keratinocyte cell line (HaCaTs) at priming doses from 0 to 20 cGy showing that the optimal priming dose is probably between 10 and 30 cGy.

Publications:

Berglund, S.R., Rocke, D.M., Dai, J., Schwietert, C., Santana, A., Stern, R., Lehman, J., Hartmann Siantar, C., and Goldberg, Z. (2007) Transient genome-wide transcriptional response to low-dose ionizing radiation in-vivo in humans, International Journal of Radiation Oncology, Biology, Physics, in press.

Susanne R. Berglund, Alison Santana, Dan Li, David Rocke, and Zelanna Goldberg, "Proteomic Analysis of Low Dose Arsenic and Ionizing Radiation Exposure on Keratinocytes," submitted for publication.

Goldberg, Z., Rocke, D., Schwietert, C., Berglund, S., Santana, A., Jones, A., Lehmann, J., Stern, R., Lu, R., Hartmann-Siantar, C. (2006) Human in vivo dose-response to controlled, low-dose low linear energy transfer ionizing radiation exposure. Clin Cancer Res., 12, 3723–3730.

Human *In vivo* Dose-Response to Controlled, Low-Dose Low Linear Energy Transfer Ionizing Radiation Exposure

Zelanna Goldberg,[1] David M. Rocke,[2] Chad Schwietert,[1] Susanne R. Berglund,[1] Alison Santana,[1] Angela Jones,[1] Jörg Lehmann,[1] Robin Stern,[1] Ruixiao Lu,[3] and Christine Hartmann Siantar[4]

Abstract

Purpose: The effect of low doses of low–linear energy transfer (photon) ionizing radiation (LDIR, <10 cGy) on human tissue when exposure is under normal physiologic conditions is of significant interest to the medical and scientific community in therapeutic and other contexts. Although, to date, there has been no direct assessment of the response of human tissue to LDIR when exposure is under normal physiologic conditions of intact three-dimensional architecture, vasculature, and cell-cell contacts (between epithelial cells and between epithelial and stromal cells).

Experimental Design: In this article, we present the first data on the response of human tissue exposed *in vivo* to LDIR with precisely controlled and calibrated doses. We evaluated transcriptomic responses to a single exposure of LDIR in the normal skin of men undergoing therapeutic radiation for prostate cancer (research protocol, Health Insurance Portability and Accountability Act–compliant, Institutional Review Board–approved). Using newly developed biostatistical tools that account for individual splice variants and the expected variability of temporal response between humans even when the outcome is measured at a single time, we show a dose-response pattern in gene expression in a number of pathways and gene groups that are biologically plausible responses to LDIR.

Results: Examining genes and pathways identified as radiation-responsive in cell culture models, we found seven gene groups and five pathways that were altered in men in this experiment. These included the Akt/phosphoinositide-3-kinase pathway, the growth factor pathway, the stress/apoptosis pathway, and the pathway initiated by transforming growth factor-β signaling, whereas gene groups with altered expression included the keratins, the zinc finger proteins and signaling molecules in the mitogen-activated protein kinase gene group. We show that there is considerable individual variability in radiation response that makes the detection of effects difficult, but still feasible when analyzed according to gene group and pathway.

Conclusions: These results show for the first time that low doses of radiation have an identifiable biosignature in human tissue, irradiated *in vivo* with normal intact three-dimensional architecture, vascular supply, and innervation. The genes and pathways show that the tissue (*a*) does detect the injury, (*b*) initiates a stress/inflammatory response, (*c*) undergoes DNA remodeling, as suggested by the significant increase in zinc finger protein gene expression, and (*d*) initiates a "pro-survival" response. The ability to detect a distinct radiation response pattern following LDIR exposure has important implications for risk assessment in both therapeutic and national defense contexts.

Although there is increasing concern and interest on the effects of low-dose low–linear energy transfer ionizing radiation (LDIR) in humans, particularly with respect to secondary radiation carcinogenesis following therapeutic radiation, there exists no direct evidence that doses in the range of 1 to 10 cGy have any biological effects whatsoever. Studies in this regard have long been stymied by ethical constraints that prohibit the intentional radiation of healthy tissue to simply examine the

Authors' Affiliations: [1]Department of Radiation Oncology, University of California Davis Cancer Center, Sacramento, [2]Division of Biostatistics, [3]Department of Statistics, University of California Davis, Davis, and [4]Lawrence Livermore National Laboratory, Livermore, California

Received 11/30/05; revised 2/18/06; accepted 3/6/06.

Grant support: Office of Biological and Environmental Research, U.S. Department of Energy (DE-FG03-01ER63237), a Campus Laboratory Collaboration grant from UCOP, the Air Force Office of Scientific Research FA955006-0132 (Z. Goldberg, S. Berglund), the National Cancer Institute grant P30 CA093373-04 (D.M. Rocke), the National Institute of Environmental Health Sciences grant P42-ES04699 (D.M. Rocke), and the University of California Davis Health Systems (D.M. Rocke). The work of C. Hartmann Siantar and J. Lehmann was performed under the auspices of the U.S. Department of Energy by the Lawrence Livermore National Laboratory under contract W-7405-ENG-48.

The costs of publication of this article were defrayed in part by the payment of page charges. This article must therefore be hereby marked *advertisement* in accordance with 18 U.S.C. Section 1734 solely to indicate this fact.

Requests for reprints: Zelanna Goldberg, Department of Radiation Oncology, University of California Davis Cancer Center, 4501 X Street, Suite G-149, Sacramento, CA 95817. Phone: 916-734-8172; Fax: 916-454-4614; E-mail: zgoldberg@ucdavis.edu.

doi:10.1158/1078-0432.CCR-05-2625

response to ionizing radiation. Attempts to address this information gap have approached the issue from two different angles.

Epidemiologic studies of exposed populations have evaluated global population exposure and health outcomes of the group, usually, although not exclusively, malignancy (1–5). A careful review of these studies reveals that, at the lowest exposure levels, no increase in detectable risk is observed. Whether this is a true threshold or simply an inherent limitation of the epidemiologic tools is the subject of vigorous debate.

The other approach to determining any potential biological activity in response to LDIR has been through classic *in vitro* cell biology, and more recently, molecular biology using genomics to characterize the response pattern. Classic end points such as cell lethality have not been sensitive enough to show any biological effects from such low dose exposures. Using genome-wide techniques on cell culture models, evidence of transcriptional changes following LDIR exposure has been shown. However, such responses are often subtle and inconsistent across models (6, 7).

Cell culture data of primary human keratinocytes and fibroblasts exposed to low or high doses of ionizing radiation have suggested a different response profile under each of these sets of circumstances (6, 7). Another group has examined brain samples from whole animal exposures and showed a transcriptomic response profile to LDIR that was qualitatively different than that seen at higher doses (8). Each of these studies has identified three distinct groups of transcripts: those that were altered by high- and low-dose exposures, those that were unique to high-dose, and those unique to the low-dose exposures. This suggests the possibility of a low-dose radiation response that is biologically dissimilar to higher doses of radiation.

While these results are intriguing, it remains unknown how applicable they are to the actual human response because the experiments were conducted on single cell layer, single cell type *in vitro* models, which fail to accommodate the known importance of cell-cell communication in radiation response. Furthermore, data suggesting that transcriptional changes of key response genes, e.g., protein kinase C, were markedly different in sensitivity and isoform when ionizing radiation was delivered *in vitro* or *in vivo* in a mouse model. This highlights the necessity for actual human data to begin assessment of the human responses to LDIR (9).

The studies described herein begin to address this information gap. We have developed a scientifically valid and ethically compliant model for direct evaluation of LDIR effects in normal human tissue, as well as a statistically validated tool to evaluate the response. Using genomic evaluation, with a priori selection of transcripts potentially sensitive to radiation-induced changes, we have (*a*) established the first data set of human responses to well-defined doses of LDIR, (*b*) developed a new methodology to address the natural heterogeneity of response in an unselected patient population, (*c*) developed a benchmark data set of transcript responses to LDIR in human skin, the first line of defense to radiation exposure from natural, medical, or terrorist sources, and (*d*) showed that although the *in vitro* evaluation of LDIR effects has identified genes and pathways activated by such exposure, it does not characterize the response in tissue. Although *in vitro* assays do serve an important role in the support of translational radiation response models, they cannot evaluate true radiation response in humans.

Materials and Methods

Patients. Men from the clinical practice of the first author, who are undergoing therapeutic radiation for the treatment of their early stage prostate cancer, were approached for possible trial participation. Informed consent was obtained (Institutional Review Board–approved, Health Insurance Portability and Accountability Act–compliant). At the time of patient treatment planning for their therapeutic ionizing radiation, an extra computed tomography scan was obtained with the patient in the treatment position. This scan was similar to the one used for therapeutic treatment planning purposes but was without any contrast material and with a slab of tissue-equivalent bolus material over the areas where biopsies were to be taken. The research scan was used for protocol treatment planning. The bolus material on the skin ensured that the region was in electronic equilibrium, reducing the radiation-absorbed dose uncertainty in the sample. The biopsy site was determined by PEREGRINE Monte Carlo dose calculations (10). On the first day of treatment, biopsy points were identified, and marked on the patient skin. TLD and/or MOSFET microdosimeters were placed on the marked sites to confirm the accuracy of the dose delivered. Biopsies were done and the samples were placed in RNAlater (Ambion, TX) until processed. Each man underwent four full skin thickness punch biopsies (3 mm diameter cores) of the normal abdominal skin. The first biopsy was prior to any ionizing radiation and served as the control sample. The other three samples were obtained 3 hours following ionizing radiation at sites determined to have received 1, 10, or 100 cGy point dose at the skin surface. Biopsies were stored at −20°C until further processing.

Tissue disruption. Each biopsy sample was loaded into a Lysing Matrix D tube (Qbiogene, Irvine, CA) containing 1 mL of a guanidine thiocyanate solution (5.1 mol/L guanidine thiocyanate, 50 mmol/L sodium citrate, 50 mmol/L EDTA, and 0.5% β-mercaptoethanol). Each sample underwent three rounds of bead beating in the Fastprep beadbeater instrument at a setting of 6 m/s (model 120A, Qbiogene). Samples were kept on ice between each pulverization step. After tissue disruption, the samples were centrifuged at 12,000 × *g* for 5 minutes at 4°C. The supernatant was removed and transferred to a new 1.5 mL Eppendorf tube.

RNA extraction and quantitation. An equal volume (1 mL) of phenol chloroform (5:1, pH 4.7) containing 0.5% *n*-lauroylsarcosine was added to each sample and incubated for 5 minutes at room temperature (Sigma, St. Louis, MO). The samples were centrifuged at 12,000 × *g* for 10 minutes at 2°C. The aqueous phase was separated from the organic phase containing DNA and protein. An additional phenol chloroform (5:1, pH 4.7) extraction was done for further purification. One milliliter of isopropanol and 200 μL of 3 mol/L sodium acetate was added to each sample for precipitation and stored overnight at −20°C. The precipitated RNA samples were cleaned up using RNeasy columns (Qiagen, CA) by following the manufacturer's cleanup procedure. Modifications to the procedure included passing the RNA through the binding column twice to increase the binding efficiency and elution of the RNA with RNA storage solution (Ambion). The Turbo DNA-Free kit was used to remove any residual DNA contamination (Ambion). RNA integrity was verified with the Molecular Devices SpectraMax plus. The RNA samples averaged 1.6 μg of total RNA and the 260:280 nm ratios were between 1.7 and 1.9. The RNA was stored at −80°C.

Amplification and labeling. The RNA was processed for the Affymetrix arrays using their one-cycle *in vitro* transcription labeling kit (Affymetrix, Santa Clara, CA). Approximately 500 μg of mRNA was reverse-transcribed using a T7-Oligo(dT) promoter primer in the first-strand synthesis. Second-strand cDNA synthesis was done and the resulting double-stranded cDNA was purified. This cDNA served as a template in the *in vitro* transcription reaction. The *in vitro* transcription reaction was carried out in the presence of T7 RNA polymerase and a biotinylated nucleotide analogue/ribonucleotide mix. The biotinylated cRNA targets were then cleaned up and fragmented using standard

Affymetrix materials and protocols. The cRNA was hybridized to the Human Genome U133 Plus 2.0 arrays.

Data set selection. To address the complexity of the data which would be generated by the Affymetrix GeneChips; a priori, we selected genes and pathways to be examined. These genes or gene pathways were chosen based on the published literature in radiation response, mostly, but not exclusively, at higher doses. To address the variable temporal response between individuals, any gene in which there was evidence in the literature to justify it as a radiation-responsive gene was evaluated, as was that entire gene pathway. This was to capture the data from all of the sample cohorts who were evaluated (biopsies obtained) at a fixed point in time after ionizing radiation exposure, recognizing that the rate of the transcriptional response would vary across the population. Below, we review the chosen genes/pathways and their rationales.

Ionizing radiation has been shown to activate nuclear factor κB through the degradation of inhibitor-κB. Therefore, the signaling pathways upstream of this (extracellular signal-regulated kinase and mitogen-activated protein kinase) were also considered in the pathways analysis (11). Cell cycle–modulating genes such as cyclins, cdc25 phosphatases, GADD45, ATM, and ATR as well as the chk-1 and chk-2 transcripts were also examined. The TP53 pathway, with upstream and downstream signaling and effector transcripts, was examined, as was transforming growth factor-β and the ubiquitons (12, 13). Growth factors, such as basic fibroblast growth factor, and its downstream targets (RAS/MEK/mitogen-activated protein kinase/RSK) were assessed, as well as other apoptosis-related paths and survival signaling pathways (Akt/phosphoinositide-3-kinase, growth factors such as tumor necrosis factor, epidermal growth factor receptor, vascular endothelial growth factor, and their downstream effectors Ras, Raf-ERK) were evaluated (14–18). DNA repair genes, in particular, the Rad 52 epistasis group, have been reported by some to be radiation-responsive, although others have questioned this relationship given the constituent expression of DNA repair proteins (6, 19). Inflammatory mediators such as cyclooxygenase-2, prostaglandin E_2, and interleukins have also been reported (20). We also selected some tissue-specific genes with structural functions (i.e., keratins) given that we anticipated some tissue reorganization in response to ionizing radiation. This type of response was reported by Ding et al. with increased expression of cytoskeleton components, ANLN and KRT15, from normal human fibroblasts (6). DNA damage/remodeling via topoisomerase and zinc finger proteins has also been reported and hence these transcripts were also examined (21) along with genes involved in cell-cell signaling, such as GRAP2 and GPR51, and cytoskeleton, such as ANLN and KRT15.

Therefore, there were seven preidentified gene pathways analyzed. They include the Akt/phosphoinositide-3-kinase pathway (14, 18, 22, 23), chemokine pathway (9, 24), fibronectin pathway (14, 24, 25), growth factor/insulin pathway (9), inflammation pathway (9, 14, 20, 22, 24, 26), stress/apoptosis pathway (9, 13, 14, 20, 22–24, 27), and the transforming growth factor-β/cyclin/ubiquitin pathway (11, 13, 14, 18, 22, 24, 25, 28). There were 19 gene groups analyzed (see Table 1).

Statistical methods. The data for this analysis consist of 32 Affymetrix HGU133 Plus 2.0 GeneChips, four from each of eight patients, at doses of 1, 10, and 100 cGy, as well as a preexposure control at 0 cGy. The HGU133 Plus 2.0 contains 1,354,896 probes divided into 54,675 probe sets, which have been summarized using the GLA expression index (29), although the results are very similar if RMA is used instead (30).

The analysis looked for dose-response patterns that were linear in dose either on the original cGy scale, or using a modified log dose (MLD) in which the positive exposures are coded as 0, 1, and 2, and the 0 exposure is coded as −1, as if it were 0.1 cGy. Because we expected (and found) variability between individuals as to timing of response on pathways and on the type of transcript within classes of genes, we did an analysis in which we aggregated results across individuals and transcripts in order to amplify possibly weak signals, without inducing false-positives.

Full details are given in Rocke (31) and Rocke et al. (32), but in summary, for each probe set and each individual, we conducted a linear regression and computed the t statistic testing for whether there is up-regulation, down-regulation, or neither. The t score will be positive if there is a trend towards up-regulation, and negative if there is an opposite trend. We examined the entire collection of t scores for a given gene group or pathway to determine the possibility of a weak signal in the direction of up-regulation or in the direction of down-regulation. We did this by testing the hypothesis that the collection of t scores had a mean of zero using the one-sample t test or a median of zero using the Wilcoxon rank-sum test. If this was rejected, it indicated that there was a trend towards up-regulation with dose of the gene group or pathway if the t scores are biased in a positive direction or towards down-regulation if the t scores are biased in a negative direction. Because of possible correlations in these test statistics, the most reliable P values are provided by resampling by repeatedly sampling random groups of transcripts of the same size. The empirical P value is the fraction of cases in the resampled gene sets in which the test statistic was more significant than the actual test statistic from the gene group or pathway. These were always two-sided P values.

Results

The Affymetrix HGU133 Plus 2.0 array platform shows the advantages and disadvantages of whole genome assays. The greatest advantage of genome-wide assays is the comprehensiveness. Not only are the genes represented on the Affymetrix chip, but each gene is represented by multiple exons. The disadvantage is that with such a large number of probe sets, there will be many apparently significant changes that occur strictly by chance, and to control for this requires a very high bar for declaring differential expression to be significant. The model that uses all 32 expression values for each probe set and tests for significant patient effects and dose-response effects would perhaps be sensitive enough if the response were highly consistent in time across individuals, but if the response is varied or diffuse, this may not yield significant results. In the 54,765 probe sets, and using the methods of Rocke (31), we found no cases in which the overall dose-response coefficient is significant at a 5% FDR level, and 11 where the FDR-adjusted significance level is better than 10% (31, 33, 34). The patient effect, however, was significant at the 5% FDR-adjusted level for 13,514 of the 54,675 probe sets, and significant at the 10% FDR-adjusted level for 18,605 of the probe sets. This shows how important the individual variation is in gene expression in radiation response. Thus, we chose to analyze the results using the methods of Rocke et al. (32) and using the gene groups and pathways identified in the literature, as described in Materials and Methods above (32).

Tables 1 and 2 show the results for the preidentified gene groups and pathways. Of the 19 gene groups, 7 have empirical $P < 0.0125$ on either the regression on dose or the regression on MLD, using either the t test or the Wilcoxon test, a number far exceeding chance (the expected number out of 19 is <1, and the probability of getting 7 significant by chance is <0.0003). The largest effects are for the BCL-6 group, keratins, protein disulfide isomerases, S100, and zinc finger proteins.

For the pathways, five of seven pathways show significant difference at the 0.0125 level in dose or MLD using either the t test or Wilcoxon test, with an expected number $\ll 1$, and the probability of having five or more significant being ~0.00006. The effect is strongly exemplified by transforming

Table 1. Results for preidentified gene groups

Gene group	No. of probe sets	Direction of effect	ToTS *t*, *P* value (dose/MLD)	ToTS W, *P* (dose/MLD)	Empirical *t*, *P* (dose/MLD)	Empirical W, *P* (dose/MLD)
BAG	9		0.1480	0.0397	0.1865	0.0460
			0.0251	0.0332	0.0195	0.0420
BCL 2	47		0.2389	0.6906	0.3410	0.7400
			0.6898	0.8323	0.7160	0.9960
BCL 6	**8**	**Up**	**0.0005**	**0.0005**	**0.0005**	**0.0000**
			0.0091	**0.0039**	**0.0035**	**0.0020**
BMPs	7		0.2181	0.2227	0.2705	0.2360
			0.5623	0.5434	0.6275	0.5440
BMP receptor	8		0.4613	0.7660	0.5320	0.7360
			0.6515	0.3828	0.6815	0.4480
Cyclins	123		0.1200	0.3530	0.2370	0.3400
			0.1347	0.2394	0.1165	0.3560
Cytokines	**86**	**Up**	**0.0169**	**0.0013**	**0.0365**	**0.0020**
			0.0184	**0.0074**	**0.0140**	**0.0260**
GADD 45	6		0.0563	0.0668	0.0555	0.0820
			0.0247	0.0380	0.0175	0.0500
Heat shock	58		0.7280	0.6620	0.7725	0.7100
			0.5784	0.3377	0.6030	0.2740
Interleukin	147		0.9877	0.4346	0.9935	0.5540
			0.6330	0.9583	0.6395	0.8080
Keratins	**101**	**Down**	**0.0020**	**7.21E-15**	**0.0070**	**0.0000**
			2.99E-14	**2.20E-16**	**0.0000**	**0.0000**
Mitogen-activated protein kinase	**131**	**Up**	**0.0020**	**0.0025**	**0.0105**	**0.0040**
			0.0143	**0.0164**	**0.0140**	**0.0440**
Protein disulfide isomerase	**8**	**Down**	**0.0139**	**0.0240**	**0.0150**	**0.0420**
			0.0121	**0.0064**	**0.0070**	**0.0000**
RAD 51	10		0.4673	0.2794	0.5340	0.3220
			0.0411	0.1495	0.0365	0.1900
S100	**21**	**Down**	**0.0144**	**0.0015**	**0.0020**	**0.0002**
			0.0001	**0.0001**	**0.0000**	**0.0000**
Serine/threonine kinase	73		0.3329	0.9555	0.4425	0.9340
			0.3778	0.9997	0.4090	0.8860
Tumor necrosis factor	109		0.8158	0.2513	0.8710	0.3520
			0.8300	0.8376	0.8505	0.6220
Topoisomerase	14		0.2022	0.1399	0.2490	0.1960
			0.0541	0.1561	0.0500	0.2520
Zinc finger	**799**	**Up**	**2.68E-05**	**7.79E-5**	**0.0135**	**0.0000**
			4.17E-06	**2.20E-16**	**0.0000**	**0.0000**

NOTE: The empirical *P* values are based on simulations of 2,000 trials for the *t* test and 1,000 trials for the Wilcoxon (W) test. Rows in bold are gene groups for which there is good evidence of differential expression. Other gene groups with borderline significance include BAG, GADD 45, RAD51, and topoisomerase. In each cell, the upper *P* value is for regression on dose, and the lower *P* value for the regression on MLD.

growth factor-β/cyclin/ubiquitin pathway activated in response to stress/apoptosis, inflammation, growth factor/insulin, and Akt/phosphoinositide-3-kinase pathways. Of the seven preidentified gene pathways analyzed, five showed a significant dose-response up-regulation to LDIR exposure. The two that did not were the chemokine and fibronectin pathways.

There were 19 gene groups analyzed, of which seven showed radiation-responsive differential gene expression. The groups that were up-regulated include BCL6 (14), cytokines (9, 23, 25, 28), mitogen-activated protein kinases (14, 20, 23, 24, 35), and zinc finger proteins (27). Those that were down-regulated include the keratins (25), the protein disulfide isomerases (15), and S100 (36). Those that did not change significantly included BAG (37), BCL2 (38), BMPs (39, 40), BMP receptors (40), cyclins (41, 42), GADD45 (43), heat shock (41, 44), interleukins (45), RAD51 (19), serine/threonine kinases (46, 47), tumor necrosis factor-β (48), and topoisomerases (21, 49). The radiation-responsive gene groups and pathways identified in our human biopsy studies have key regulatory roles in cell cycle arrest, DNA repair, inflammation, and apoptosis.

Table 2. Results for preidentified pathways

Pathway	No. of probe sets	Direction of effect	ToTS *t*, *P* (dose/MLD)	ToTS W, *P* (dose/MLD)	Empirical *t*, *P* (dose/MLD)	Empirical W, *P* (dose/MLD)
Akt/phosphoinositide-3-kinase pathway	**99**	**Up**	**0.0014**	**0.0002**	**0.0050**	**0.0020**
			0.1333	**0.0006**	**0.1335**	**0.0020**
Chemokine pathway	79		0.2716	0.4047	0.3895	0.4780
			0.8565	0.2649	0.8730	0.4080
Fibronectin pathway	196		0.0206	0.0649	0.0990	0.1020
			0.0497	0.0169	0.0455	0.0460
Growth factor/insulin pathway	**208**	**Up**	**0.0001**	**0.0072**	**0.0015**	**0.0100**
			0.5044	**0.0083**	**0.5405**	**0.0220**
Inflammation pathway	**78**	**Up**	**0.0365**	**0.0013**	0.0785	**0.0020**
			0.0687	**0.1187**	**0.0810**	**0.1780**
Stress/apoptosis pathway	**151**	**Up**	**0.9343**	**0.0739**	**0.9500**	**0.0400**
			0.0359	**0.0029**	**0.0420**	**0.0070**
Transforming growth factor-β/ cyclin/ubiquitin pathway	**355**	**Up**	**0.0003**	**0.0005**	**0.0095**	**0.0000**
			0.0014	**0.0012**	**0.0005**	**0.0010**

NOTE: The empirical *P* values are based on simulations of 2,000 trials for the *t* test and 1,000 trials for the Wilcoxon (W) test. Rows in bold are pathways for which there is good evidence of differential expression. In each cell, the upper *P* value is for regression on dose, and the lower *P* value for the regression on MLD.

In most cases, gene groups and pathways that were significant over all patients were also significant for individual patients, although this did not always occur, which is consistent with the assumption of interindividual variability in response. In many cases, the individual tests were not significant, consistent with the lower statistical power of a test based on one individual, and in only a few cases was the effect significant in the opposite direction. This overall consistency gives additional confidence in the realism of the results. Details are given in Table 3.

As noted above in Materials and Methods, all expression data were analyzed using a model of linear dose-response. Thus, significant results indicate linear response in expression up (or down) with dose over the range of 1 to 100 cGy. Those gene groups or pathways that were not statistically significant on a linear model had variable responses across dose and could not be modeled by a linear fit.

The microarray data from this study are available in Minimum Information About a Microarray Gene Experiment–compliant format from the National Center for Biotechnology Information Gene Expression Omnibus repository and include the 32. CEL files and the probe set summary data for all 32 arrays and 54,675 probe sets in a Microsoft Excel file, as well as the experimental metadata. The data sets defining the gene groups and pathways, and the programs in the R language that were used to process the data are available as supplementary files from the Journal web site. All of these files are also available on the second author's web site, http://www.idav.ucdavis.edu/~dmrocke.

Table 3. Results for individual patients for significant gene groups and pathways

Gene group or pathway	Direction of effect	No. of patients up-regulated	No. of patients down-regulated	No. of patients not significant
BCL 6	Up	4	0	4
Cytokines	Up	3	1	4
Keratins	Down	8	0	3
Mitogen-activated protein kinase	Up	2	0	6
Protein disulfide isomerase	Down	0	2	6
S100	Down	0	3	5
Zinc finger	Up	6	1	1
Akt/phosphoinositide-3-kinase pathway	Up	5	0	3
Growth factor/insulin pathway	Up	4	0	4
Inflammation pathway	Up	4	1	3
Stress/apoptosis pathway	Up	3	1	4
Transforming growth factor-β/cyclin/ubiquitin pathway	Up	3	0	5

Discussion

Ionizing radiation is a naturally ubiquitous toxicant. Background radiation is now supplemented through most peoples' lives by industrial exposures and medical exposures for diagnostic and/or therapeutic reasons. Furthermore, in the era of intensity-modulated radiation therapy, larger volumes of normal tissue are exposed to low doses of ionizing radiation. There is also a newly elevated threat from radiologic terrorism, driving the need to determine the biological effects, if any, of low levels of radiation exposure in the human.

By devising a dosimetrically sound sampling method on individuals who are otherwise healthy but receiving therapeutic localized radiation for early stage prostate cancer, we have developed a new model system whereby direct evaluation of radiation effects can be determined. This model is ethically sound, Institutional Review Board–approved, and allows real-time sampling of human tissue after *in vivo* radiation exposures of precisely calibrated radiation doses. This model is therefore unique in allowing the evaluation of whole tissue effects when exposure is under normal physiologic conditions.

Biopsies were obtained from patients 3 hours after an acute exposure to LDIR. This time point was chosen for practical considerations. More recently, emerging data have shown that low dose-response may be better defined at a later time point (6, 7, 35). Although none of the published data have examined an *in vivo* human model, it is reasonable to question whether a greater response may be seen after a longer interval. If so, this would suggest that secondary tissue effects, i.e., cellular responses to signaling from neighboring cells may be as important in tissue response to LDIR as the initial radiation deposition within the cells. Studies to better characterize the temporal response to LDIR in tissue, in a separate cohort of men, are ongoing and will be reported separately.

Using genome-wide analysis, preselected targeted genes, and pathways from *in vitro* studies, we have shown that human skin initiates a transcript program to enhance survival whereas simultaneously undergoing an inflammatory and stress response. Whether these pathways are all activated in the same cells within the tissue, or represent responses from different tissues (i.e., epithelial versus stromal versus vasculature) cannot be determined from this data set. Laser capture dissection of the biopsied tissue for separate analysis of each cell type can be undertaken now that benchmark data have been compiled showing that low-dose ionizing radiation is biologically active in a definable way in the human. These data were analyzed on the assumption of a linear dose-response. Nonlinearity at the lowest doses cannot be excluded.

The tissues sampled and examined were evaluated as whole tissue. Therefore, the genomic signature is a summative evaluation of the responses of thousands of cells of several lineages, containing both epithelial and stromal cells. Some of the cells would represent lineages that are classically "radiation-sensitive" whereas others were radiation-resistant. Although this model does not allow precise mechanistic intervention, it does offer a comparative advantage in giving us tissue level response which will be the defining level of human response—i.e., the tissue level response is more than just the summative whole of individual cell responses. The doses examined in this study, and those of interest to the radiation risk community are well below those that are frankly cytotoxic. Therefore, the tissue response will inevitably be an amalgamation of the primary response of the cell and the modulating effects of the cells surrounding it, both of the same lineage and others. This amalgamated response therefore incorporates the bystander response and represents the organismal response to the radiation insult. Aside from better determining the extent of true human response to low doses of ionizing radiation, it also provides a potential biosignature for evaluating skin exposure to low doses of ionizing radiation, well below doses expected to produce symptomatic radiation effects.

We have devised a methodology whereby an individual biopsy from these same sample types can be processed for both RNA and protein with both collected for analysis. This will allow a matched genomic and proteomic evaluation.[5] These evaluations are ongoing, but will further extend our ability to define the tissue level response of human skin to low doses of ionizing radiation.

Defining the effects of low-dose radiation in humans requires a model with diverse genetic background with the subsequent statistical tool development to identify the effect of the agent above the background diversity of the study population. Therefore, we did these benchmark studies on an otherwise unselected population and devised statistically rigorous tools to address human complexity. Limitations of a sample set consisting of males with early stage prostate cancer are a clear lack of gender diversity and a limited age range. Radiation sensitivities in other populations, specifically the young and fetus' *in utero*, cannot be extrapolated from these data. This data set included samples from six Caucasians and two African-Americans.

The skin forms the first barrier of the body to radiation exposure and is an easy tissue to biopsy for scientific evaluation, clinical studies and potential field application for population screening for radiation exposure. It is a dynamic, complex system with multiple cell types. Because only healthy skin was biopsied (not previous scars or cancerous lesions), this radiation profile may represent a generalizable biosignature. The age distribution within the patient population sampled does not allow an analysis of age effects, and, as noted above, gender effects cannot be excluded. Relating this transcriptomic signature to a functional tissue end point for human health is part of an ongoing project.

These benchmark data show for the first time that low doses of radiation have an identifiable biosignature in human tissue, irradiated *in vivo* with normal intact three-dimensional architecture, vascular supply, and innervation. The genes and pathways show that the tissue (*a*) detects the injury, (*b*) initiates a stress/inflammatory response, (*c*) undergoes DNA remodeling, suggested by the significant increase in genes for zinc finger proteins being expressed, and (*d*) initiates a "pro-survival" response.

Acknowledgments

We thank the patients who volunteered and all of the radiation therapists in the Department of Radiation Oncology, University of California Davis Cancer Center, UCDHS. The authors are grateful for the helpful comments from the referees of the original version of this article.

[5] Berglund S.R., Schwietert C.W., Jones A., Stern R.L., Lehmann J., and Goldberg Z. Optimized methodology for dual extraction of RNA and protein from small human skin biopsy, submitted for publication.

References

1. Boice J, Jr. Study of health effects of low-level radiation in USA nuclear shipyard workers. J Radiol Prot 2001;21:400–3.
2. Brooks AL. Developing a scientific basis for radiation risk estimates: goal of the DOE Low Dose Research Program. Health Phys 2003;85:85–93.
3. Cohen BL. Test of the linear no-threshold theory of radiation carcinogenesis in the low dose, low dose rate region. Health Phys 1995;68:157–74.
4. Ghiassi-nejad M, Mortazavi SM, Cameron JR, Niroomand-rad A, Karam PA. Very high background radiation areas of Ramsar, Iran: preliminary biological studies. Health Phys 2002;82:87–93.
5. Kostyuchenko VA, Krestinina L. Long-term irradiation effects in the population evacuated from the east Urals radioactive trace area. Sci Total Environ 1994;142: 119–25.
6. Ding LH, Shingyoji M, Chen F, et al. Gene expression profiles of normal human fibroblasts after exposure to ionizing radiation: a comparative study of low and high doses. Radiat Res 2005;164:17–26.
7. Franco N, Lamartine J, Frouin V, et al. Low-dose exposure to γ rays induces specific gene regulations in normal human keratinocytes. Radiat Res 2005; 163:623–35.
8. Yin E, Nelson DO, Coleman MA, Peterson LE, Wyrobek AJ. Gene expression changes in mouse brain after exposure to low-dose ionizing radiation. Int J Radiat Biol 2003;79:759–75.
9. Varadkar PA, Krishna M, Verma NC. Dose-dependent differential expression of protein kinase C isozymes in mouse lymphocytes after γ irradiation *in vivo* and *ex vivo*. Radiat Res 2003;159:453–7.
10. Lehmann J, Stern RL, Daly TP, et al. Dosimetry for quantitative analysis of low dose ionizing radiation effects on humans in radiation therapy patients. Radiat Res 2006;165:240–7.
11. Li N, Karin M. Ionizing radiation and short wavelength UV activate NF-κB through two distinct mechanisms. Proc Natl Acad Sci U S A 1998;95:13012–7.
12. Barcellos-Hoff MH. How tissues respond to damage at the cellular level: orchestration by transforming growth factor-{β} (TGF-{β}). BJR Suppl 2005;27: 123–7.
13. MacCallum DE, Hall PA, Wright EG. The Trp53 pathway is induced *in vivo* by low doses of γ radiation. Radiat Res 2001;156:324–7.
14. Gu Q, Wang D, Wang X, et al. Basic fibroblast growth factor inhibits radiation-induced apoptosis of HUVECs. II. The RAS/MAPK pathway and phosphorylation of BAD at serine 112. Radiat Res 2004;161:703–11.
15. Prasad SC, Soldatenkov VA, Kuettel MR, et al. Protein changes associated with ionizing radiation-induced apoptosis in human prostate epithelial tumor cells. Electrophoresis 1999;20:1065–74.
16. Sartor CI. Epidermal growth factor family receptors and inhibitors: radiation response modulators. Semin Radiat Oncol 2003;13:22–30.
17. Shonai T, Adachi M, Sakata K, et al. MEK/ERK pathway protects ionizing radiation-induced loss of mitochondrial membrane potential and cell death in lymphocytic leukemia cells. Cell Death Differ 2002;9: 963–71.
18. Sartor C. Mechanisms of disease: radiosensitization by epidermal growth factor receptor inhibitors. Nat Clin Pract Oncol 2004;1:22–30.
19. Bishay K, Ory K, Olivier MF, et al. DNA damage-related RNA expression to assess individual sensitivity to ionizing radiation. Carcinogenesis 2001;22: 1179–83.
20. Tessner TG, Muhale F, Schloemann S, et al. Ionizing radiation up-regulates cyclooxygenase-2 in I407 cells through p38 mitogen-activated protein kinase. Carcinogenesis 2004;25:37–45.
21. Forrester HB, Radford IR. Ionizing radiation-induced chromosomal rearrangements occur in transcriptionally active regions of the genome. Int J Radiat Biol 2004;80:757–67.
22. Dent P, Yacoub A, Contessa J, et al. Stress and radiation-induced activation of multiple intracellular signaling pathways. Radiat Res 2003;159:283–300.
23. Kumar P, Miller AI, Polverini PJ. p38 MAPK mediates γ-irradiation-induced endothelial cell apoptosis, and vascular endothelial growth factor protects endothelial cells through the phosphoinositide 3-kinase-Akt-Bcl-2 pathway. J Biol Chem 2004;279:43352–60.
24. Lee SA, Dritschilo A, Jung M. Impaired ionizing radiation-induced activation of a nuclear signal essential for phosphorylation of c-Jun by dually phosphorylated c-Jun amino-terminal kinases in ataxia telangiectasia fibroblasts. J Biol Chem 1998;273:32889–94.
25. Kim AH, Lebman DA, Dietz CM, et al. Transforming growth factor-β is an endogenous radioresistance factor in the esophageal adenocarcinoma cell line OE-33. Int J Oncol 2003;23:1593–9.
26. Zimmermann JS, Kumpf L, Kimmig B. Variability of individual normal tissue radiation sensitivity. An international empirical evaluation of endogenous and exogenous response modifiers. Strahlenther Onkol 1998;174:16–9.
27. Ahmed MM. Regulation of radiation-induced apoptosis by early growth response-1 gene in solid tumors. Curr Cancer Drug Targets 2004;4:43–52.
28. Pajonk F, McBride WH. Ionizing radiation affects 26s proteasome function and associated molecular responses, even at low doses. Radiother Oncol 2001; 59:203–12.
29. Zhou L, Rocke D. An expression index for Affymetrix GeneChips based on the generalized logarithm. Bioinformatics 2005;21:3983–9.
30. Irizarry RA, Bolstad BM, Collin F, et al. Summaries of Affymetrix GeneChip probe level data. Nucleic Acids Res 2003;31:e15.
31. Rocke DM. Design and analysis of experiments with high throughput biological assay data. Semin Cell Dev Biol 2004;15:708–13.
32. Rocke DM, Goldberg Z, Schweitert C, Santana A. A method for detection of differential gene expression in the presence of inter-individual variability in response. Bioinformatics 2005;21:3990–2.
33. Reiner A, Yekutieli D, Benjamini Y. Identifying differentially expressed genes using false discovery rate controlling procedures. Bioinformatics 2003;19: 368–75.
34. Benjamini Y, Hochberg Y. Controlling the false discovery rate—a practical and powerful approach to multiple testing. J R Stat Soc Ser B-Methodological 1995;57:289–300.
35. Amundson SA, Fornace AJ, Jr. Monitoring human radiation exposure by gene expression profiling: possibilities and pitfalls. Health Phys 2003;85:36–42.
36. El-Naaman CG-SB, Mansouri A, Grigorian M, et al. Cancer predisposition in mice deficient for the metastasis-associated Mts1 (S100A4) gene. Oncogene 2004;23:3670–80.
37. Chen X, Shen B, Xia L, et al. Activation of nuclear factor κB in radioresistance of TP53-inactive human keratinocytes. Cancer Res 2002;62:1213–21.
38. An J, Xu QZ, Sui JL, Bai B, Zhou PK. Silencing of DNA-PKcs alters the transcriptional profile of certain signal transduction genes related to proliferation and differentiation in HeLa cells. Int J Mol Med 2005;16: 455–62.
39. Lee JH, Lee YM, Park JW. Regulation of ionizing radiation-induced apoptosis by a manganese porphyrin complex. Biochem Biophys Res Commun 2005;334: 298–305.
40. Pohl F, Hassel S, Nohe A, et al. Radiation-induced suppression of the Bmp2 signal transduction pathway in the pluripotent mesenchymal cell line C2C12: an *in vitro* model for prevention of heterotopic ossification by radiotherapy. Radiat Res 2003; 159:345–50.
41. Shankar B, Sainis KB. Cell cycle regulators modulating con A mitogenesis and apoptosis in low-dose radiation-exposed mice. J Environ Pathol Toxicol Oncol 2005;24:33–43.
42. Pond CD, Leachman SA, Warters RL. Accumulation, activation and interindividual variation of the epidermal TP53 protein in response to ionizing radiation in organ cultured human skin. Radiat Res 2004;161:739–45.
43. Snyder AR, Morgan WF. Gene expression profiling after irradiation: clues to understanding acute and persistent responses? Cancer Metastasis Rev 2004;23: 259–68.
44. Kang CM, Park KP, Cho CK, et al. Hspa4 (HSP70) is involved in the radioadaptive response: results from mouse splenocytes. Radiat Res 2002;157:650–5.
45. Rho HS, Park SS, Lee CE. γ Irradiation up-regulates expression of B cell differentiation molecule CD23 by NF-κB activation. J Biochem Mol Biol 2004;37:507–14.
46. Contessa JN, Hampton J, Lammering G, et al. Ionizing radiation activates Erb-B receptor dependent Akt and p70 S6 kinase signaling in carcinoma cells. Oncogene 2002;21:4032–41.
47. Khodarev NN, Park JO, Yu J, et al. Dose-dependent and independent temporal patterns of gene responses to ionizing radiation in normal and tumor cells and tumor xenografts. Proc Natl Acad Sci U S A 2001;98: 12665–70.
48. Zeise E, Weichenthal M, Schwarz T, Kulms D. Resistance of human melanoma cells against the death ligand TRAIL is reversed by ultraviolet-B radiation via downregulation of FLIP. J Invest Dermatol 2004;123: 746–54.
49. Agner J, Falck J, Lukas J, Bartek J. Differential impact of diverse anticancer chemotherapeutics on the Cdc25A-degradation checkpoint pathway. Exp Cell Res 2005;302:162–9.

Title: Proteomic Analysis of Low Dose Arsenic and Ionizing Radiation Exposure on Keratinocytes

Authors: Susanne R. Berglund[1], Alison Santana[1], Dan Li[2], David Rocke[3] and Zelanna Goldberg[1,*]

[1]Department of Radiation Oncology, University of California Davis Cancer Center, 4501 X Street, Sacramento, CA, USA, 95817

[2]Graduate Group in Applied Mathematics, University of California Davis, Davis, 1 Shields Avenue, CA, USA, 95616

[3]Division of Biostatistics, University of California Davis, 1 Shields Avenue, Davis, CA, USA, 95616

Running Title: Analysis of Low Dose Arsenic/IR Exposure on Keratinocytes

*Corresponding author:

Zelanna Goldberg

Dept. of Radiation Oncology

UC Davis Cancer Center

2700 Stockton Blvd, #1108

Sacramento CA 95817

Phone: (916) 734-7421

Fax: (916) 457-4306

zgoldberg@ucdavis.edu

Abbreviations:

As	sodium arsenite
CaM	calmodulin
E-FABP	epidermal fatty acid-binding protein
HINT-1	histidine triad nucleotide-binding protein 1
HSP27	heat shock protein 27
IR	ionizing radiation
LDH-A	lactate dehydrogenase A
PDI	protein disulfide isomerase precursor

Summary

While the human health effects of arsenic and ionizing radiation have been examined separately, there is little information regarding their interactions at low doses approaching environmental levels. The idea of synergistic toxicity is a well-known phenomenon in human disease. Arsenic toxicity may be affected at low dose exposure by concurrent ionizing radiation especially in light of their known individual carcinogenic actions at higher doses.

We employed a proteomics approach in a human keratinocyte cell line to examine the interaction of ionizing radiation and arsenic. Toxicant exposure resulted in differential proteomic expression based on immunoblotting and statistical analysis (ANOVA) of identified proteins.

Thirteen proteins were identified including: annexin XI, calmodulin, cyclophilin A, α-enolase, epidermal fatty acid-binding protein, heat shock protein 27, histidine triad nucleotide-binding protein 1, lactate dehydrogenase A, profilin-1, protein disulfide isomerase precursor, pyruvate kinase M isozyme, R3372_1 and S100A9.

Six proteins responded to ionizing radiation and eight reacted to arsenic exposure. Four proteins, α-enolase, epidermal fatty acid binding protein, lactate dehydrogenase A and protein disulfide isomerase, had an interaction effect that was different than would be expected based on the effects of either toxicant alone. These data demonstrate a possible response to the combined insult that is substantially different from either separate treatment. The response of α-enolase and protein disulfide isomerase were dissimilar from what has been found using higher doses, adding to the idea that cellular response to low dose exposures are distinct from the responses to

high dose exposures. This study begins to address the cellular proteomic response to low dose exposures of dual environmental toxicants.

Introduction

Low level arsenic and low dose ionizing radiation are both environmental toxicants. While data exist which examine the human health effects of either toxicant separately, there are no data in the literature regarding possible interactions at low doses. Yet, interactions of toxicants to produce synergistic toxicity is a well-known phenomenon in human disease (e.g. radon/tobacco or arsenic/tobacco smoke in lung cancer induction) [1, 2]. Additionally, the FDA has approved the use of low levels of arsenic to treat acute promyelocytic leukemia. With the growing use of IMRT, which results in an increase in healthy tissue exposed to low dose ionizing radiation, the possibility of receiving a combined or sequential exposure to these particular toxicants in a medical setting requires further biologic characterization [3]. Arsenic toxicity may be affected at low dose exposure levels by concurrent ionizing radiation especially in light of their known carcinogenic actions individually at higher doses. Prior studies that examine each substance independently suggest the possibility of overlapping cellular defense pathways which are activated by the toxicants [4-7].

Arsenic is a naturally occurring metalloid that can be solubilized in water under certain conditions, posing the threat of contaminated drinking water [8, 9]. It has been well documented that exposure to arsenic can contribute to skin, bladder, liver and lung cancers [8, 10-13]. While the mechanisms of arsenic toxicity are still not fully understood, several ideas have been postulated

including induction of oxidative stress, decreased functioning of DNA repair systems, chromosomal abnormality and altered growth factors [14-16]. There is evidence that exposure to arsenic generates an oxidative stress response which can cause an increase in the presence of reactive oxygen species (ROS) [13, 14]. Exposure of cells to ROS can have many effects, including DNA damage and mutation [17]. Changes in DNA repair may occur by changing the expression of genes involved in the synthesis of DNA repair enzymes, rendering cells unable to fix damaging mutations [13, 18]. This mechanism has also been proposed as an explanation to arsenic's co-mutagenic effects [19].

Ionizing radiation (IR) exposure is unavoidable in the environment and further exposure is commonly obtained through medical imaging. Average background radiation in the United States is 360 mrem (whole body equivalent exposure) with medical imaging exposures adding up to 5 cGy focal absorbed dose. There is substantial debate regarding the biological effects of low dose IR in humans and no direct information on how such exposure may alter the response of cells to other environmental toxicants [20-22]. As with arsenic, IR exerts the majority of its toxicity through the intracellular generation of ROS. The ROS affect the target cell, as well as generating a redox sensitive signal to surrounding cells, the so-called bystander effect [23]. It is therefore plausible that oxidative stress induced from IR could substantially enhance the effects of otherwise minimally toxic, sublethal exposures of arsenic.

Much remains uncertain about the effects of these toxicants at low doses. Historically, most radiation studies have involved high dose exposures with the assumption that the toxicant profile could be extrapolated down in a linear manner for low dose exposures. This is the

underlying assumption in the linear no-threshold model of radiation effects, which is currently undergoing challenge (as reviewed in: [24-27]). Doubt still remains regarding the biological effects of low dose IR on humans, how the effects are exerted and the shape of the low dose IR response curve [22].

As with IR exposure, much remains unknown about the dose response curve for low level arsenic exposure. In the past, it was assumed that the response for high doses of arsenic could also be applied to low dose exposures [9]. However, current studies have yet to demonstrate a direct relationship between low dose arsenic exposure and cancer, suggesting a nonlinear relationship and supporting the idea that the dose response curve at low levels can not be inferred from high dose studies [13]. Thus, as there is no accepted, comprehensive model describing the mechanism by which low dose toxin exposures exert their effects, there is no predictive modeling that can address the potential interacting effects of co-exposures on cells. Therefore, direct empiric study remains the cornerstone of understanding potential interactions and how the co-exposures may alter the safety profile of each.

The skin is the major barrier to many environmental toxicants, with keratinocytes being the most prevalent cell type. Arsenic exposure can lead to many diseases of the skin, while IR exposures generally penetrate the skin. Chronic arsenic exposure often leads to hyperpigmentation, hyperkeratosis and arsenic induced Bowen's disease [15]. In time, Bowen's disease can progress into invasive skin cancer in the form of basal or squamous cell carcinoma [15]. Keratinocytes are readily cultivated and respond to toxicant and other damaging challenges

with changes in transcription up to 10%, making them an ideal model for this study [5]. Further, this model has already been used for both sublethal arsenic and low dose IR studies [5, 25, 28].

Our investigation begins to address the gap in the toxicology literature regarding potential interactions of low level toxicant exposures. It has been shown that transcriptional changes within the cell do not correlate completely with translational studies [29-32]. Few studies have focused on the proteomic differences induced by these toxicants and this study begins to address the lack of proteomic data and provides complementary information to transcriptional data. As proteins are the components through which a cell enacts change, the differences found in the proteome may better reflect the actual cellular response of significance for human health outcomes. Using a proteomics approach in a human keratinocyte model to mimic human skin exposure, we examined the interaction of ionizing radiation and arsenic.

Experimental Procedures

Cell Culture

A spontaneously immortalized human keratinocyte (SIK) cell line was grown with a lethally irradiated feeder layer of 3T3 cells obtained from ATCC #48-X (ATCC, VA) [5]. Cells were supported with a 3:1 mixture of Dulbecco-Vogt Eagle and Ham's F-12 media containing 5% fetal bovine serum, 0.4 μg/ml hydrocortisone, 5 μg/ml insulin, 5 μg/ml transferrin, 20 pM triiodothyronine, 0.18 mM adenine, 10 ng/ml cholera toxin and 10 ng/ml epidermal growth factor [5]. Cell medium was changed every 3 days.

Arsenic and IR Treatment

Once cells reached near confluency, half of the flasks were treated with medium containing 2 μM sodium arsenite. At 24 hours, flasks were irradiated with x-rays at low doses of 1 or 10 cGy. Tissue culture flasks were irradiated with a Varian 2100C on a 30 x 30 cm^2 acrylic block with a tissue equivalent bolus covering the top of the flasks to ensure accuracy of dose delivery. Dose rate was set at 80 cGy/min, and SSD was 101.3 cm (1 cGy) or 100 cm (10 cGy). Radiation free controls were maintained with and without sodium arsenite. One or four days post irradiation, flasks were rinsed with 0.02% EDTA in phosphate buffered saline to remove residual 3T3 cells. All samples were prepared in triplicate. Flasks were held at -80° C until protein extraction.

Protein Extraction

Flasks were removed from -80°C freezer and thawed to room temperature. One ml of Mammalian Protein Extraction Reagent (MPER, Pierce Biotechnology, IL) containing 1:100 protease inhibitor (Sigma-Aldrich, MO) was added to each flask, cells were scraped and lysate was transferred to a 2 ml tube on ice. Each sample was sonicated for 1 min and centrifuged at 10,000 x *g* for 20 minutes at 4°C. Supernatant was removed and placed in a clean 2 ml tube. Protein quantitation was performed using Coomassie Plus Protein Assay (Pierce Biotechnology, IL).

2D electrophoresis

Isoelectric focusing was performed using a Protean IEF Cell (Bio-Rad, CA). A 30 μg aliquot of the protein was combined with a lysis buffer solution (0.5% Triton X-100, 4% CHAPS, 7 M urea, 2 M thiourea, nanopure water), 1% Biolyte 3-10 buffer, 2% protease inhibitor cocktail (Calbiochem, CA), 0.065% dithiothreitol and a trace amount of bromophenol blue dye for a total volume of 200 μl. The solubilized protein samples were left at room temperature for one hour before loading. ReadyStrip IPG strips (pH 3-10, 11cm) were used for separation in the first dimension (Bio-Rad, CA).

Isoelectric focusing was conducted at 20°C using the following voltage program: 50 V for a 12-hour rehydration period; 50-250 V linear ramp; 250-8000 V linear ramp; hold (total 42 kVh). After focusing, the strips were incubated in an equilibration buffer (5 ml consisting of 50 mM Tris, pH 8.8, 6 M urea, 30% glycerol, 2% SDS, trace bromophenol blue and 0.065% ditheothreitol (DTT)) for 15 minutes on a rocking platform. The strips were subsequently incubated with the same equilibration buffer substituting 10 mM iodoacetamide for DTT to alkylate cysteine sulfhydryls. The strips were then placed on top of 12% SDS Duracryl gels and sealed using 0.5% agarose (Genomic Solutions, MI).

The second dimension separation was performed in a Hoefer SE 600/SE 660 2D-PAGE system interfaced to a Powerpac 3000 power supply (Bio-Rad, CA). Gels were run in an SDS tank buffer (25mM Tris, 192 mM glycine, 0.1% SDS) at 15 mA per gel for 30 minutes followed by 25 mA per gel until the dye migrated to the bottom of the gel. Broad range Precision Plus Protein Standard plug molecular weight protein markers were used for mass calibration of the

gels (10-250 kDa) (Bio-Rad, CA). Gels were fixed in 10% acetic acid, 40% methanol, and 50% water, silver stained and scanned with an Epson Perfection 4870 photo scanner.

Image analysis

The 36 gel images were processed with analysis software Progenesis (PG240 v2006) and TT900 S2S (Nonlinear Dynamics, UK). Gel images were first warped with TT900 S2S. Warped images were then imported to Progenesis for further analysis including: spot detection, spot matching, background subtraction, spot filtering and 'Samespot Outline'. The Samespot Outline in Progenesis copies spot outlines from gels where a spot exists to those gels missing the spot, then calculates the spot volume within the new outlines. Therefore all missing values are filled with calculated volumes. There were 2,002 individual proteins recognized on each gel with Progenesis (PG240 v2006, Nonlinear Dynamics, UK).

Protein digestion and mass spectrometry

The Nevada Proteomics Center analyzed selected proteins by trypsin digestion and MALDI TOF/TOF analysis. Gel pieces were destained using reagents from the Silver Quest – Silver staining kit (Invitrogen, CA, cat# LC6070). Spots were digested using a previously described protocol with some modifications [33]. Samples were washed twice with 25 mM ammonium bicarbonate (ABC) and 100% acetonitrile, reduced and alkylated using 10 mM DTT and 100 mM iodoacetamide and incubated with 75 ng sequencing grade modified porcine trypsin (Promega, WI) in 25 mM ABC for 6 hours at 37°C. Samples were spotted onto a MALDI target with ZipTipμ-C18 (Millipore Corp., MA). Samples were eluted with 70% acetolnitrile, 0.2%

formic acid and overlaid with 0.5 µl 5 mg/ml MALDI matrix (α-Cyano-4 hydroxycinnamic acid, 10 mM ammonium phosphate). All mass spectrometric data were collected using an ABI 4700 Proteomics Analyzer MALDI TOF/TOF mass spectrometer (Applied Biosystems, CA), using their 4000 Series Explorer software v. 3.6. The peptide masses were acquired in reflectron positive mode (1-keV accelerating voltage) from a mass range of 700 – 4000 Daltons and either 1250 or 2500 laser shots were averaged for each mass spectrum. Each sample was internally calibrated on trypsin's autolysis peaks 842.51 and 2211.10 to within 20 ppm. Any sample failing to internally calibrate was analyzed under default plate calibration conditions of 150 ppm. Raw spectrum filtering/peak detection settings were S/N threshold of 3, and cluster area S/N optimization enabled at S/N threshold 10, baseline subtraction enabled at peak width 50. The eight most intense ions from the MS analysis, which were not on the exclusion list, were subjected to tandem mass spectrometry. The MS/MS exclusion list included known trypsin masses along with unidentified background peaks: 842.51, 856.52, 870.54, 1011.65, 1045.56, 1126.56, 1338.83, 1666.01, 1794.9, 1940.94, 2211.10, 2225.12, 2283.18 and 3094.62. For MS/MS analysis the mass range was 70 to precursor ion with a precursor window resolution of 50 FWHM (full-width at half maximum) with an average 2500 laser shots for each spectrum, CID on, metastable suppressor on. Raw spectrum filtering/peak detection settings were S/N threshold of 5, and cluster area S/N optimization enabled at S/N threshold 6, baseline subtraction enabled at peak width 50. The data was then stored in an Oracle database (Oracle database schema v. 3.19.0, Data version 3.90.0).

MALDI data analysis

The data was extracted from the Oracle database and a peak list was created by GPS Explorer software v 3.6 (Applied Biosystems) from the raw data generated from the ABI 4700. Analyses were performed as combination mass spectrometry and tandem mass spectrometry. MS peak filtering included mass range 700-4000 Da, minimum S/N filter 10, mass exclusion tolerance of 0.2 Da. Exclusion list of known trypsin fragments and unidentified background peaks: 2211.2, 2283.2, 1045.6, 842.5, 1794.9, 1011.65, 1338.83, 1666.01. A peak density filter of 50 peaks per 200 Da with a maximum number of peaks set to 65. MS/MS peak filtering included mass range of 60 Da to 20 Da below each precursor mass. Minimum S/N filter 5, peak density filter of 50 peaks per 200 Da, cluster area filter used with maximum number of peaks 65. The filtered data were searched by Mascot v 1.9.05 (Matrix Science) using CDS combined database (Celera Discovery System v. KBMS3.2.20040119), containing 1,416,555 sequences. Searches were performed without restriction to protein species, M_r, or pI and with variable oxidation of methionine residues and carbamidomethylation of cysteines (no fixed modifications). Maximum missed cleavage was set to 1 and limited to trypsin cleavage sites. Precursor mass tolerance and fragment mass tolerance were set to 20 ppm and ± 0.2 Da, respectively. Protein hits with high confidence identifications and statistically significant search scores, greater than 95% confidence interval (C.I.%) or $p \leq 0.05$, were accepted. High confidence identifications were consistent with the protein experimental M_r, and pI and the majority of the ions present in the mass spectra were accounted for.

Immunoblot analysis

Western blots were performed for sequenced proteins that had high confidence identification and which had available commercial antibodies. Protein samples (10 μg) were

separated on 12%, Ready Gel Tris-HCl precast gels (BioRad, CA). Proteins were electroblotted to PVDF membrane and blocked overnight at 4°C. Primary antibodies were pyruvate kinase (ab6191, Abcam, MA), α-enolase (sc-15343, Santa Cruz Biotechnology, CA), S100A9 (sc-8114, SCB, CA), PDI (sc-30932, SCB, CA), profilin-1 (sc-18346, SCB, CA), annexin XI (sc-9322, SCB, CA), E-FABP (sc-16060, SCB, CA), and LDH-A (sc-27230, SCB, CA), cytokeratin 1 (sc-17091, SCB, CA), CaM (sc-1989, SCB, CA), HSP27 (sc-1048, SCB, CA), HINT-1 (10717-1-AP, Proteintech Group, IL) and cyclophilin A (10720-1-AP, Proteintech Group , IL). All primary antibodies were used at 0.2 μg/ml final concentration, typically a 1:1000 dilution. The secondary antibody (donkey anti-goat-hrp, sc-2020 or donkey anti-rabbit, sc-2004, SCB, CA) was used at a 1:40,000 dilution. Membranes were developed in ECL Advanced (GE Healthcare, NJ) and images were captured on a ChemiDoc system with Quantity One software (BioRad, CA). A monoclonal antibody to β-actin was used as a loading control and all density readings were normalized (sc-47778, SCB, CA). Western blots were performed in triplicate. The western blot data were analyzed using ANOVA after normalization by β-actin.

Statistical Analysis

Statistical differential analyses consisted of data preprocessing, analysis of variance (ANOVA), adjusting for multiple hypothesis testing and the chi-square test. Statistical methods are often based on the assumption that data are normally distributed with constant variance not dependent on the mean; therefore, it is important to preprocess the data so that they do not violate these assumptions. In this case preprocessing consisted of logarithmic transformation and mean-centering normalization. The analysis of variance model was applied to identify differentially expressed proteins with effects for the level of arsenic, the level of IR, and the

interaction effect. Two methods of estimating the protein-specific variance in ANOVA were utilized, the usual mean square for error and an estimate adjusted by an empirical Bayes method originally developed for microarrays [34, 35] (manuscript in progress, Dan Li).

Results

Image and Statistical Analysis

Proteins were isolated from keratinocytes that had been exposed to 0 or 2 μM sodium arsenite and 0, 1 or 10 cGy of irradiation for one or four days. These proteins were separated using two-dimensional gel electrophoresis. All conditions were run in triplicate and the resulting 36 gels were imaged and analyzed. The initial analysis included keratinocytes exposed to a 1 cGy irradiation dose. Little differential expression was detected with this low dose and these samples were omitted from the final analysis.

ANOVA was performed on the each of 2,002 spots detected at each time point individually. Proteins that displayed significant ($p \leq 0.05$) differential expression (after correction for multiple comparisons) using either ANOVA method were selected as candidates for sequencing, resulting in 444 spots identified for further characterization.

Mass Spectrometry and Protein Identification

Protein spots were chosen for sequencing only if they were distinct, outside of areas with background smearing and could be removed from the gel without excising other nearby proteins. A total of 24 samples were sent to the Nevada Proteomics Center for analysis, nine spots from day one and fifteen from day four (figure 1). Thirteen proteins with a protein score

CI% above 95% were identified by mass spectrometry and tandem mass spectrometry (table 1). The proteins identified by mass spectrometry and tandem mass spectrometry from the 24 hour time point included: calmodulin (CaM), heat shock protein 27 (HSP27), lactate dehydrogenase A (LDH-A) and protein disulfide isomerase precursor (PDI, synonym: thyroid hormone binding protein precursor) (figure 2). The proteins found four days post exposure included: annexin XI (annexin XI), S100A9 (synonym: calgranulin B), cyclophilin A (synonym: peptidyl-prolyl cis-trans isomerase), α-enolase, epidermal fatty acid binding protein (E-FABP), histidine triad nucleotide-binding protein 1 (HINT-1), profilin-1, pyruvate kinase M isozyme, and R3372_1 (a protein fragment) (figure 3).

Immunoblotting

Twelve identified proteins had available commercial antibodies and were selected for immunoblotting (table 2). This was done as an important cross-check on the ANOVA analysis for the 2D gels. Given the complexity of the required statistical analysis for the 2D gels, it is always possible that some spots identified as differentially expressed were in fact artifactual. CaM was not recognized by the antisera in detectable amounts and no protein band was verified at the appropriate molecular weight. This does not exclude the possibility that CaM may have been differentially expressed since western blots require a relatively high concentration for detection. For the eleven remaining proteins, the β-actin-normalized intensity data determined (table 3). These data were analyzed using ANOVA (table 4). Eight of the eleven proteins (E-FABP, α-enolase, HINT-1, HSP27, LDH-A, PDI, cyclophilin A, and S100A9) showed significant ($p < 0.05$) differences for either IR, As, or the interaction, which far exceeds the chance rate (roughly one or two false significance values could be expected out of the 11

proteins by chance alone). Three showed no significant difference at the $p < 0.05$ level (annexin XI, pyruvate kinase and profilin-1). The HSP27 was down regulated and HINT-1 was up regulated in response to individual treatments, though neither protein showed an interaction effect that was significantly different than either single treatment. Cyclophilin A, E-FABP, PDI and S100A9 decreased with exposure to arsenic. Both E-FABP and LDH-A showed a response to the combined insult that was greater than would have been expected from either treatment alone, while α-enolase and PDI had a response that was less than would be expected from the individual exposures.

Discussion

Low dose ionizing radiation and low levels of arsenic are environmental toxins and below a certain threshold, their individual toxicity is believed to be minimal. However the effects of combining these two known carcinogens at these doses are unknown. As a model for low dose toxicant interaction, they are of significant interest as irradiation is ubiquitous and arsenic, although heavily regulated in the US, is still a major environmental burden in many countries. There is little in the scientific literature examining human health risks associated with possible toxicant interactions despite the known synergy of such agents in malignancy [1, 2, 15, 36]. Thus, these data serve to begin to fill this information gap.

Of the twelve proteins selected for immunoblotting, eight showed significant differences in protein expression and three yielded inconsistent results (annexin XI, pyruvate kinase and profilin-1). It is possible that the expression changes detected by the ANOVA of the gel images

were too small to be detected by western blotting given its semi-quantitative nature. All proteins with variable results had faint spots on the 2D gels indicating a very low protein concentration as silver staining can detect nanogram quantities of protein, a sensitivity beyond that of western blotting.

Proteins that were immunoblotted included three proteins from the early time point: PDI, LDH-A and HSP27. None of these proteins were found at the later time point indicating a transient response. At four days post exposure, E-FABP, α-enolase, S100A9, HINT-1 and cyclophilin A had altered expression. Doses examined in this study are much lower than those that are clearly cytotoxic and this proteomic response implies that the cells are actively responding to low-level exposures.

Our data adds to and confirms several prior studies using these toxicants. PDI, a stress response protein was down regulated in a previous study by exposure to arsenic [5]. We found this protein was down regulated in response to both arsenic and arsenic plus IR. The LDH isoenzyme spectrum in human serum changes following radiation exposure, tumor development, as well as in response to disease [37-39]. The isoform LDH-A is typically found to be down regulated in response to these stressors. This protein was identified as significantly down regulated in response to the combined exposure. However, the western blot images and the normalized density readings show that the LDH-A appears to be down regulated in response to both treatments individually, but these results were not statistically significant.

This study revealed that the interaction effect of IR with arsenic significantly down regulated α-enolase. Enolase is multifunctional and can serve as a plasminogen-binding receptor, a stress protein, a structural protein, a glycolytic enzyme and a transcriptional repressor [40, 41]. Wu et al reported that cells treated with all-trans retinoic acid (a suppressor of cellular growth and differentiation) showed a two-fold decrease in α -enolase levels in hepatocarcinoma cells and suggested that α-enolase is down regulated in slow growth conditions [42]. Interestingly, a study by Tallman et al shows that the use of all-trans retinoic acid in the treatment of patients with acute promyelocytic leukemia results in increased survival [43]. α-enolase is known to have higher expression in many tumor types and has been shown to be hypoxia inducible, however caution must be used when extrapolating results from cancerous tissues and cell lines to normal human keratinocytes [44, 45]. It has been postulated that α-enolase is critical to tumor invasion and metastasis via activation of the plasminogen system [41]. While no firm conclusions can be drawn, this interaction of low dose IR and low dose arsenic in α-enolase expression does suggest that further study is warranted given the postulated role in malignant behavior and in light of current cancer therapies.

Expression of the S100A9 protein was significantly down regulated by the arsenic or the combination treatment. S100A9 is one of a family of S100 proteins found in a wide variety of cells and involved in calcium signal transduction, cell cycle progression and cellular differentiation, especially in keratinocytes and epidermal tissues [46]. Two microarray analyses on the effects of low dose ionizing radiation (0-100 cGy) on full thickness human skin show that, as a large family, the S100 gene group is down regulated within the first 24 hours [5, 26, 47]. Another recent proteomic analysis of laryngeal cancer found decreased expression in the S100A9 protein

as compared to nearby healthy tissue [48]. To our knowledge, there are no reports on S100A9 arsenic altered expression.

E-FABP was significantly down regulated by arsenic and up regulated by the combined exposure. E-FABP has an affinity for binding to fatty acids and is involved in keratinocyte differentiation, synthesis of phospholipids and has a role as an antioxidant which scavenges reactive lipids [49, 50]. E-FABP is known to interact with S100A7 and these proteins are up regulated in psoriasis and certain cancers [51, 52]. In prior genomic studies, S100A9 and E-FABP have been shown to be up regulated in response to tissue damage [53, 54]. While these interactions need to be clarified, our data adds supports the possibility that these two proteins, S100A9 and E-FABP, may interact with one another.

Two proteins yielded variable immunoblotting results, pyruvate kinase M1/M2 isozyme and cyclophilin A. The polyclonal pyruvate kinase antibody was not specific for the M isoform. A shift in the pyruvate kinase isozyme profile from tissue specific pyruvate kinase to the M2 form is an indication of early carcinogenesis and the conformational shifting of M2 from tetrameric to dimeric isoform occurs in late carcinogenesis [55-57]. The ANOVA analysis of cyclophilin A revealed a significant response with exposure to arsenic. Cyclophilin A is involved in Ca^{2+} ion signaling and when complexed with cyclosporin A it inhibits calcineurin, a calcium/calmodulin phosphatase [58]. We identified calmodulin and PDI regulation upon exposure to arsenic, while a prior study of the response of keratinocytes to arsenic identified calcineurin, all of which are involved in Ca^{2+} ion signaling [5, 58].

Both IR and arsenic dose responses are currently based on the idea of a linear no-threshold model [13, 24]. Many studies are revealing that low dose exposures are fundamentally different from high dose exposures [25, 26]. For example, it has been shown that α-enolase was up regulated in-vivo with a high dose exposure of 9 Gy, whereas our study did not confirm this trend [59]. Prasad et al showed that a dose of 6 Gy of irradiation led to increases in the protein levels of PDI, calreticulin and calnexin in apoptotic cells 48 hours post exposure. Low dose exposure of 2 μM arsenic alone or with 10 cGy IR diminished cellular amounts of both PDI and calreticulin [5]. These results suggest that the response to low doses of irradiation and arsenic may be substantially different than those seen following higher dose exposures. A response pattern of that type would be consistent with emerging data from other studies dealing with low dose IR and low dose arsenic [5, 26, 47].

Several of the identified proteins were found to have a response to the combined exposure that was different from the response to either toxicant individually, including E-FABP, α-enolase, LDH-A and PDI. These data demonstrate a possible response to the combined insult that is significantly different than either treatment alone, making them candidates for further study as potential biomarkers. Many of the proteins found in this study are currently recognized as biomarkers of disease processes. Pyruvate kinase M2 is a biomarker for colorectal cancer, while a change in the usual LDH isozyme spectrum is indicative of ischemia, radiation treatment or cancer, while S100A9 has been found as a serum component after radiation [38, 60, 61]. The identification of biomarkers in conjunction with changing isozyme spectra that is unique to a combination of environmental toxicants may lead to novel detection panels for suspected

environmental toxicant exposures. With these findings, we have begun the process of identifying potential biomarkers of these types of combined exposures.

This study examined near background levels of arsenic and IR to determine the potential for overlapping cellular responses. Previous work has shown that arsenic exposure alters the expression of heat shock proteins, annexin and PDI, while IR has been reported to alter heat shock protein 60, annexin and PDI, as well as α-enolase [4, 6, 59]. Our research indicates that HINT-1 and HSP27 respond in the same manner to either arsenic or IR. Other proteins (E-FABP, α-enolase, LDH-A and PDI) had an effect that was significantly different than would be expected based on a single exposure. These proteomic responses are consistent with the idea that cellular defenses to environmental toxicants have partially overlapping response pathways, suggesting the possibility that the alteration of two minimally toxic, sublethal exposures may combine into a lethal or carcinogenic response.

Acknowledgments

We would like to acknowledge that the first and second authors have made equal contributions to this work. We would like to thank Dr. Robert Rice at the Department of Environmental Toxicology at University of California, Davis and Dr. Karen Kalanetra at the UC Davis Medical Center for their helpful discussions and critical reviews of this manuscript. We would also like to thank Rebekah Woolsey at Nevada Proteomic Center for her technical expertise. This work was supported by grants from a Campus Laboratory Collaboration Grant 2003-2004 from UCOP (ZG), the Air Force Office of Scientific Research FA9550-06-1-0132 and FA9550-07-1-0146 (ZG, SB, and DMR), National Cancer Institute P30 CA093373-04 (DMR), National Human Genome Research Institute R01-HG003352 (DMR), National Institute of Environmental Health Sciences P42-ES04699 (DMR), UC Davis Health Systems (DMR). The Nevada Proteomics Center is supported by NIH Grant Number P20 RR-016464 from the INBRE Program of the National Center for Research Resources.

References

1. Hertz-Picciotto, I., Smith, A. H., Holtzman, D., Lipsett, M., Alexeeff, G. (1992) Synergism between occupational arsenic exposure and smoking in the induction of lung cancer. *Epidemiology.* 3, 23-31.
2. Pershagen, G., Wall, S., Taube, A., Linnman, L. (1981) On the interaction between occupational arsenic exposure and smoking and its relationship to lung cancer. *Scand J Work Environ Health.* 7, 302-309.
3. Ivanov, V. N., Zhou, H., Hei, T. K. (2007) Sequential treatment by ionizing radiation and sodium arsenite dramatically accelerates TRAIL-mediated apoptosis of human melanoma cells. *Cancer Res.* 67, 5397-5407.
4. Gehrmann, M., Marienhagen, J., Eichholtz-Wirth, H., Fritz, E., Ellwart, J., Jaattela, M., Zilch, T., Multhoff, G. (2005) Dual function of membrane-bound heat shock protein 70 (Hsp70), Bag-4, and Hsp40: protection against radiation-induced effects and target structure for natural killer cells. *Cell Death Differ.* 12, 38-51.
5. Lee, C., Lee, Y. M., Rice, R. H. (2005) Human epidermal cell protein responses to arsenite treatment in culture. *Chem Biol Interact.* 155, 43-54.
6. Prasad, S. C., Soldatenkov, V. A., Kuettel, M. R., Thraves, P. J., Zou, X., Dritschilo, A. (1999) Protein changes associated with ionizing radiation-induced apoptosis in human prostate epithelial tumor cells. *Electrophoresis.* 20, 1065-1074.
7. Tokalov, S. V., Pieck, S., Gutzeit, H. O. (2007) Varying responses of human cells with discrepant p53 activity to ionizing radiation and heat shock exposure. *Cell Prolif.* 40, 24-37.
8. Nordstrom, D. K. (2002) Public health. Worldwide occurrences of arsenic in ground water. *Science.* 296, 2143-2145.
9. Ahsan, H., Chen, Y., Parvez, F., Zablotska, L., Argos, M., Hussain, I., Momotaj, H., Levy, D., Cheng, Z., Slavkovich, V., van Geen, A., Howe, G. R., Graziano, J. H. (2006) Arsenic Exposure from Drinking Water and Risk of Premalignant Skin Lesions in Bangladesh: Baseline Results from the Health Effects of Arsenic Longitudinal Study. *Am J Epidemiol.*
10. Brown, K. G., Ross, G. L. (2002) Arsenic, drinking water, and health: a position paper of the American Council on Science and Health. *Regul Toxicol Pharmacol.* 36, 162-174.
11. Guha Mazumder, D. N., Haque, R., Ghosh, N., De, B. K., Santra, A., Chakraborty, D., Smith, A. H. (1998) Arsenic levels in drinking water and the prevalence of skin lesions in West Bengal, India. *Int J Epidemiol.* 27, 871-877.
12. Shi, H., Hudson, L. G., Ding, W., Wang, S., Cooper, K. L., Liu, S., Chen, Y., Shi, X., Liu, K. J. (2004) Arsenite causes DNA damage in keratinocytes via generation of hydroxyl radicals. *Chem Res Toxicol.* 17, 871-878.
13. Schoen, A., Beck, B., Sharma, R., Dube, E. (2004) Arsenic toxicity at low doses: epidemiological and mode of action considerations. *Toxicology and Applied Pharmacology.* 198, 253-267.
14. Kitchin, K. T. (2001) Recent advances in arsenic carcinogenesis: modes of action, animal model systems, and methylated arsenic metabolites. *Toxicol Appl Pharmacol.* 172, 249-261.
15. Yu, H. S., Liao, W. T., Chai, C. Y. (2006) Arsenic carcinogenesis in the skin. *J Biomed Sci.* 13, 657-666.

16. Reichard, J. F., Schnekenburger, M., Puga, A. (2007) Long term low-dose arsenic exposure induces loss of DNA methylation. *Biochem Biophys Res Commun.* 352, 188-192.
17. Valko, M., Rhodes, C. J., Moncol, J., Izakovic, M., Mazur, M. (2006) Free radicals, metals and antioxidants in oxidative stress-induced cancer. *Chem Biol Interact.* 160, 1-40.
18. Hamadeh, H. K., Trouba, K. J., Amin, R. P., Afshari, C. A., Germolec, D. (2002) Coordination of altered DNA repair and damage pathways in arsenite-exposed keratinocytes. *Toxicol Sci.* 69, 306-316.
19. Vogt, B. L., Rossman, T. G. (2001) Effects of arsenite on p53, p21 and cyclin D expression in normal human fibroblasts -- a possible mechanism for arsenite's comutagenicity. *Mutat Res.* 478, 159-168.
20. Amundson, S. A., Do, K. T., Fornace, A. J., Jr. (1999) Induction of stress genes by low doses of gamma rays. *Radiat Res.* 152, 225-231.
21. Goldberg, Z., Schwietert, C. W., Lehnert, B., Stern, R., Nami, I. (2004) Effects of low-dose ionizing radiation on gene expression in human skin biopsies. *Int J Radiat Oncol Biol Phys.* 58, 567-574.
22. Sagan, L. A., Cohen, J. J. (1990) Biological effects of low-dose radiation: overview and perspective. *Health Phys.* 59, 11-13.
23. Goldberg, Z., Lehnert, B. E. (2002) Radiation-induced effects in unirradiated cells: a review and implications in cancer. *Int J Oncol.* 21, 337-349.
24. Ding, L. H., Shingyoji, M., Chen, F., Hwang, J. J., Burma, S., Lee, C., Cheng, J. F., Chen, D. J. (2005) Gene expression profiles of normal human fibroblasts after exposure to ionizing radiation: a comparative study of low and high doses. *Radiat Res.* 164, 17-26.
25. Franco, N., Lamartine, J., Frouin, V., Le Minter, P., Petat, C., Leplat, J. J., Libert, F., Gidrol, X., Martin, M. T. (2005) Low-dose exposure to gamma rays induces specific gene regulations in normal human keratinocytes. *Radiat Res.* 163, 623-635.
26. Goldberg, Z., Rocke, D. M., Schwietert, C., Berglund, S. R., Santana, A., Jones, A., Lehmann, J., Stern, R., Lu, R., Hartmann Siantar, C. (2006) Human in vivo dose-response to controlled, low-dose low linear energy transfer ionizing radiation exposure. *Clin Cancer Res.* 12, 3723-3729.
27. Yin, E., Nelson, D. O., Coleman, M. A., Peterson, L. E., Wyrobek, A. J. (2003) Gene expression changes in mouse brain after exposure to low-dose ionizing radiation. *Int J Radiat Biol.* 79, 759-775.
28. Bernstam, L., Lan, C. H., Lee, J., Nriagu, J. O. (2002) Effects of arsenic on human keratinocytes: morphological, physiological, and precursor incorporation studies. *Environ Res.* 89, 220-235.
29. Chen, G., Gharib, T. G., Huang, C. C., Taylor, J. M., Misek, D. E., Kardia, S. L., Giordano, T. J., Iannettoni, M. D., Orringer, M. B., Hanash, S. M., Beer, D. G. (2002) Discordant protein and mRNA expression in lung adenocarcinomas. *Mol Cell Proteomics.* 1, 304-313.
30. Dongre, A. R., Opiteck, G., Cosand, W. L., Hefta, S. A. (2001) Proteomics in the post-genome age. *Biopolymers.* 60, 206-211.
31. Gygi, S. P., Rochon, Y., Franza, B. R., Aebersold, R. (1999) Correlation between protein and mRNA abundance in yeast. *Mol Cell Biol.* 19, 1720-1730.

32. Zhai, R., Su, S., Lu, X., Liao, R., Ge, X., He, M., Huang, Y., Mai, S., Lu, X., Christiani, D. (2005) Proteomic profiling in the sera of workers occupationally exposed to arsenic and lead: identification of potential biomarkers. *Biometals.* 18, 603-613.
33. Rosenfeld, J., Capdevielle, J., Guillemot, J. C., Ferrara, P. (1992) In-gel digestion of proteins for internal sequence analysis after one- or two-dimensional gel electrophoresis. *Anal Biochem.* 203, 173-179.
34. Rocke, D. M. (2004) Design and analysis of experiments with high throughput biological assay data. *Semin Cell Dev Biol.* 15, 703-713.
35. Wright, G. W., Simon, R. M. (2003) A random variance model for detection of differential gene expression in small microarray experiments. *Bioinformatics.* 19, 2448-2455.
36. Klein, C. B., Leszczynska, J., Hickey, C., Rossman, T. G. (2007) Further evidence against a direct genotoxic mode of action for arsenic-induced cancer. *Toxicol Appl Pharmacol.*
37. Klimov, I. A., Serdiukov, A. S., Elistratova, N. B. (1989) [Lactate dehydrogenase isoenzymes in radiation therapy of cancer patients]. *Lab Delo.* 16-17.
38. Nagasue, N. (1975) Changes in lactic dehydrogenase isoenzymes after hepatic artery ligation in patients with hepatic carcinoma. *Gastroenterol Jpn.* 10, 150-156.
39. Singh, R., Kaurya, O. P., Shukla, P. K., Ramputty, R. (1991) Lactate dehydrogenase (LDH) isoenzymes patterns in ocular tumours. *Indian J Ophthalmol.* 39, 44-47.
40. Jeffery, C. J. (2003) Moonlighting proteins: old proteins learning new tricks. *Trends Genet.* 19, 415-417.
41. Pancholi, V. (2001) Multifunctional alpha-enolase: its role in diseases. *Cell Mol Life Sci.* 58, 902-920.
42. Wu, N., Zhang, W., Yang, Y., Liang, Y. L., Wang, L. Y., Jin, J. W., Cai, X. M., Zha, X. L. (2006) Profilin 1 obtained by proteomic analysis in all-trans retinoic acid-treated hepatocarcinoma cell lines is involved in inhibition of cell proliferation and migration. *Proteomics.* 6, 6095-6106.
43. Tallman, M. S., Andersen, J. W., Schiffer, C. A., Appelbaum, F. R., Feusner, J. H., Ogden, A., Shepherd, L., Willman, C., Bloomfield, C. D., Rowe, J. M., Wiernik, P. H. (1997) All-trans-retinoic acid in acute promyelocytic leukemia. *N Engl J Med.* 337, 1021-1028.
44. Ishiguro, Y., Kato, K., Ito, T., Horisawa, M., Nagaya, M. (1984) Enolase isozymes as markers for differential diagnosis of neuroblastoma, rhabdomyosarcoma, and Wilms' tumor. *Gann.* 75, 53-60.
45. Katayama, M., Nakano, H., Ishiuchi, A., Wu, W., Oshima, R., Sakurai, J., Nishikawa, H., Yamaguchi, S., Otsubo, T. (2006) Protein pattern difference in the colon cancer cell lines examined by two-dimensional differential in-gel electrophoresis and mass spectrometry. *Surg Today.* 36, 1085-1093.
46. Eckert, R. L., Broome, A. M., Ruse, M., Robinson, N., Ryan, D., Lee, K. (2004) S100 proteins in the epidermis. *J Invest Dermatol.* 123, 23-33.
47. Berglund S. R., Rocke, D. M., Dai J., Schwietert C. W., Santana A. R., Stern R. L., Lehmann J., Hartmann Siantar C. L. and Goldberg Z. (2007, accepted) Transient Genome-Wide Transcriptional Response to Low-Dose Ionizing Radiation In-Vivo in Humans. *IJROBP.*

48. Sewell, D. A., Yuan, C. X., Robertson, E. (2006) Proteomic Signatures in Laryngeal Squamous Cell Carcinoma. *ORL J Otorhinolaryngol Relat Spec.* 69, 77-84.
49. Grau, V., Garn, H., Holler, J., Rose, F., Blocher, S., Hirschburger, M., Fehrenbach, H., Padberg, W. (2006) Epidermal fatty acid-binding protein is increased in rat lungs following in vivo treatment with keratinocyte growth factor. *Int J Biochem Cell Biol.* 38, 279-287.
50. Urschitz, J., Iobst, S., Urban, Z., Granda, C., Souza, K. A., Lupp, C., Schilling, K., Scott, I., Csiszar, K., Boyd, C. D. (2002) A serial analysis of gene expression in sun-damaged human skin. *J Invest Dermatol.* 119, 3-13.
51. Fujii, K., Kondo, T., Yokoo, H., Yamada, T., Iwatsuki, K., Hirohashi, S. (2005) Proteomic study of human hepatocellular carcinoma using two-dimensional difference gel electrophoresis with saturation cysteine dye. *Proteomics.* 5, 1411-1422.
52. Siegenthaler, G., Hotz, R., Chatellard-Gruaz, D., Jaconi, S., Saurat, J. H. (1993) Characterization and expression of a novel human fatty acid-binding protein: the epidermal type (E-FABP). *Biochem Biophys Res Commun.* 190, 482-487.
53. Gerke, V., Creutz, C. E., Moss, S. E. (2005) Annexins: linking Ca2+ signalling to membrane dynamics. *Nat Rev Mol Cell Biol.* 6, 449-461.
54. Tomas, A., Moss, S. E. (2003) Calcium- and cell cycle-dependent association of annexin 11 with the nuclear envelope. *J Biol Chem.* 278, 20210-20216.
55. Kaura, B., Bagga, R., Patel, F. D. (2004) Evaluation of the Pyruvate Kinase isoenzyme tumor (Tu M2-PK) as a tumor marker for cervical carcinoma. *J Obstet Gynaecol Res.* 30, 193-196.
56. Mazurek, S., Boschek, C. B., Hugo, F., Eigenbrodt, E. (2005) Pyruvate kinase type M2 and its role in tumor growth and spreading. *Semin Cancer Biol.* 15, 300-308.
57. Shastri, Y. M., Naumann, M., Oremek, G. M., Hanisch, E., Rosch, W., Mossner, J., Caspary, W. F., Stein, J. M. (2006) Prospective multicenter evaluation of fecal tumor pyruvate kinase type M2 (M2-PK) as a screening biomarker for colorectal neoplasia. *Int J Cancer.* 119, 2651-2656.
58. Kahl, C. R., Means, A. R. (2003) Regulation of cell cycle progression by calcium/calmodulin-dependent pathways. *Endocr Rev.* 24, 719-736.
59. Zhang, B., Su, Y. P., Ai, G. P., Liu, X. H., Wang, F. C., Cheng, T. M. (2003) Differentially expressed proteins of gamma-ray irradiated mouse intestinal epithelial cells by two-dimensional electrophoresis and MALDI-TOF mass spectrometry. *World J Gastroenterol.* 9, 2726-2731.
60. Ewald, N., Toepler, M., Akinci, A., Kloer, H. U., Bretzel, R. G., Hardt, P. D. (2005) [Pyruvate kinase M2 (tumor M2-PK) as a screening tool for colorectal cancer (CRC). A review of current published data]. *Z Gastroenterol.* 43, 1313-1317.
61. Pandit, M. K., Joshi, B. H., Patel, P. S., Chitnis, K. E., Balar, D. B. (1990) Efficacy of serum lactate dehydrogenase and its isozymes in monitoring the therapy in patients with acute leukemia. *Indian J Pathol Microbiol.* 33, 41-47.

Figure Legends

Table 1

Protein identification. Proteins identified from mass spectrometry and tandem mass spectrometry. Fields include: spot number as displayed in figure 1, protein name, accession number from CDScombined database (Celera Discovery System v. KBMS3.2.20040119), MASCOT protein score, MASCOT ion score, protein and ion score confidence indices, species of protein hit, and protein molecular weight, pI, peptide count and total amino acid sequence coverage. Also shown are the matched peptides and corresponding masses, mass errors, sequences and number of unmatched sequences if protein ion score is less than 100. Peptides analyzed by tandem mass spectrometry display ion scores and confidence indices.

Table 2

Immunoblot images of proteins identified by MS/MS. Immunoblots were performed for each selected protein. 10 μg of protein were separated, transferred to PVDF, and developed using ECL Advanced reagent. Images were captured on a ChemiDoc system. (A) control sample (B) IR only, (C) As only and (D) IR plus As. Each immunoblot was performed in triplicate and images shown are representative of all blots performed. Each blot was probed for β-actin as a loading control and one representative image is shown.

Table 3

Western blot density data. The average intensity per mm^2 was determined for each band using Quantity One software. The intensity data from each protein were normalized to the β-actin

data. Cyclophilin A yielded variable results with immunoblotting, but was shown to have a significant response to arsenic in the ANOVA analysis. The data from three replicates blots are given.

Table 4

Significant effects in the ANOVA of the western blot analysis. The p-value is given for all effects significant at the 0.05 level. The (↑) symbol in the IR or As column indicates that the given protein is up regulated upon treatment with the respective toxicant, and the (↓) symbol indicates down regulation. For the IR*As interaction, the (+) symbol indicates that the protein expression is greater than would have been expected from the two stimuli independently, and (–) indicates that the protein expression is less than would have been expected. In general, we can conclude that there has been evidence of an IR perturbation of protein expression if either the IR or the IR*As effect is significant, and that there has been evidence of an As perturbation if either the As or IR*As effect is significant. Thus 6 of the 11 proteins showed a reaction to IR, 8 of the 11 showed a reaction to As (including all that showed a reaction to IR), and 3 were inconclusive. The ANOVA was performed for all exposures, — indicates no significant change.

Figure 1

Figure 1 Two dimensional gels with labeled protein spot numbers selected for analysis. Keratinocytes were treated with low dose arsenic and ionizing radiation and protein was isolated one or four days post exposure. Numbered spots were excised and sent to the Nevada Proteomic Center for identification.

Figure 2

MS spectrum of proteins identified at the 24 hours time point. The images are annotated in color to correspond with the MASCOT results. (A) CaM, (B) HSP27, (C) LDH-A and (D) PDI. Red annotation denotes a direct match to the protein in MASCOT, blue indicates submission to MASCOT with no match. Masses shown in black were excluded from the MASCOT search as they were a trypsin peak, a known contaminant or the S/N was lower than the threshold.

Figure 3

MS spectrum of proteins identified fours days post IR treatment. The images are annotated in color to correspond with the MASCOT results. (A) annexin XI, (B) cyclophilin A, (C) α-enolase, (D) HINT-1, (E) E-FABP (spot 2611), (F) E-FABP (spot 2640), (G) profilin-1, (H) pyruvate kinase M isozyme, (I) R3372_1 and (J) S100A9. Red annotation is a match to the protein hit in MASCOT, blue labeling indicate submission to MASCOT with no match. Black indicates masses excluded from the MASCOT search as they were trypsin peaks, known contaminants or the S/N was lower than the threshold.